3-Dimensional Echocardiography in Aortic Valve Repair

13. September 2018
Saarland University Medical Center - Homburg/Saar, Germany

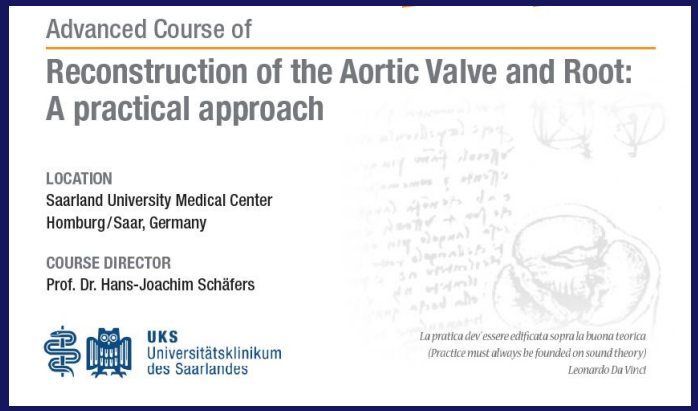

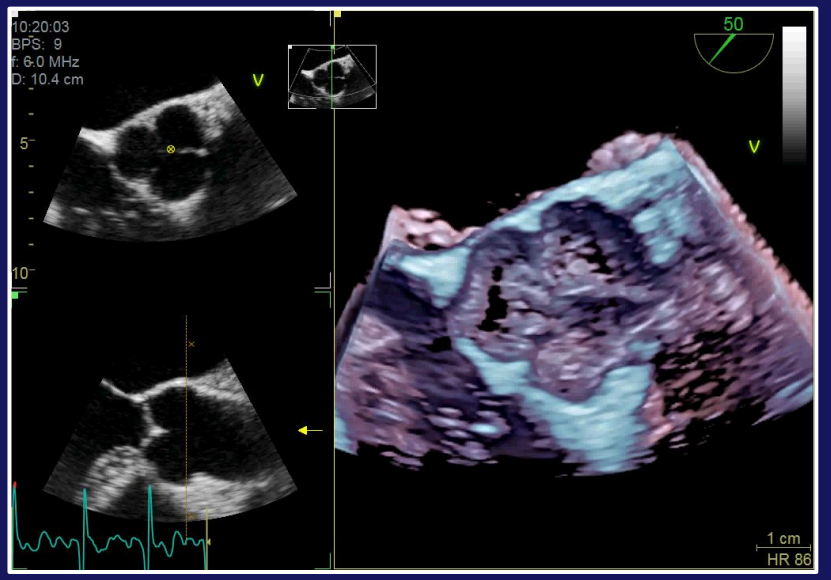

Prof. Dr. med. Andreas Hagendorff,
Universitätsklinikum Leipzig
Klinik für Kardiologie
Liebigstraße 20 - 04103 Leipzig
Andreas.Hagendorff@medizin.uni-leipzig.de

Advanced Course of Reconstruction of the Aortic Valve and Root: A Practical Approach

EBAC
Declaration of Interests Policy and Rules

I declare for the last 3 years and the subsequent 12 month the following conflicts of interests:

Section I: Support for Research Activities
- grant of the DEGUM
- no other financial research support

Section II: Support for Educational Activities
- MIFO, GE Healthcare, Astra Zeneca, Servier, Novartis, Berlin-Chemie, Pfizer, Cardiac Dimension, Abbott, Bayer, Canon, Kelcon

Section III: Honorarium for Promotional Activities - none

Section IV: Personal Financial Interests in Vommercial Activities - none

IB1; 2A11
Member of the German Society of Cardiology,
the German Society of Ultrasound DEGUM), the German Society of Internal Medicine and the European Society of Cardiology/Cardiovascular Imaging
Secretary of the DEGUM Board

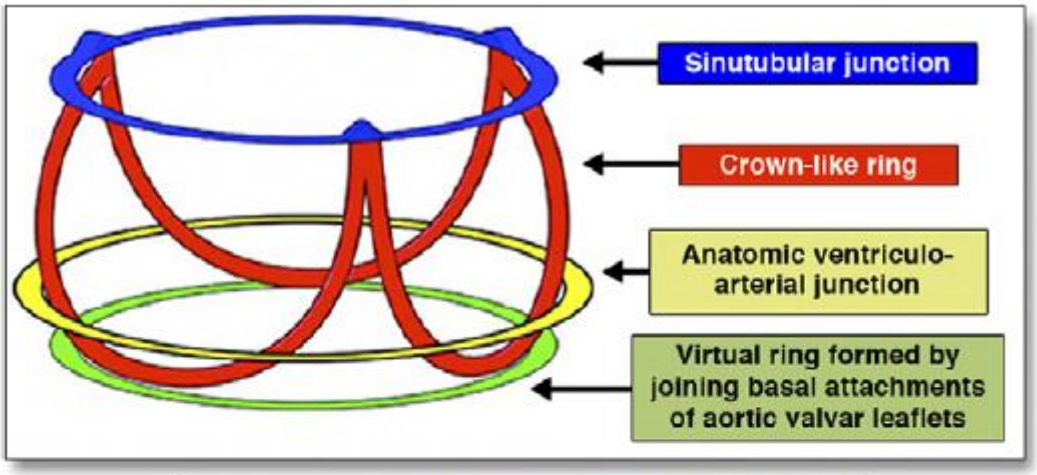

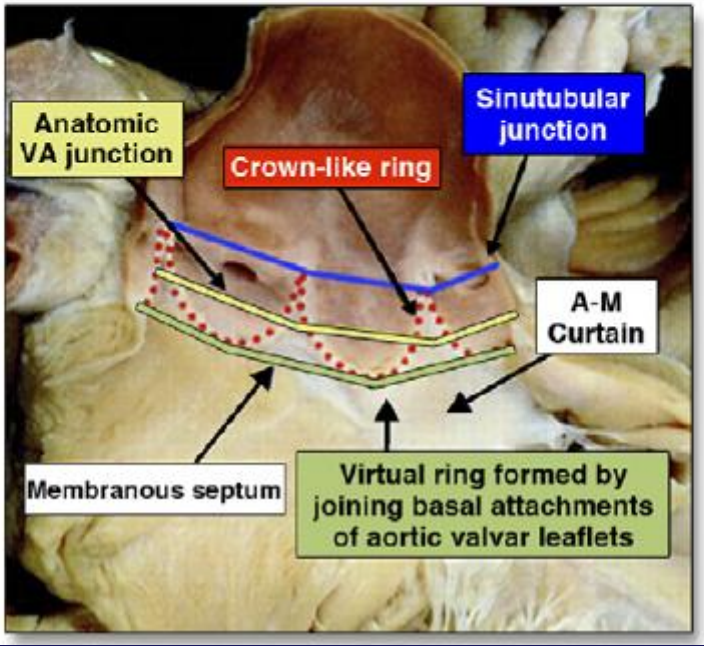

Aortic Root Anatomy
(A) Diagram of aortic root anatomy showing coronet shape and location of various annular planes and coronary ostia relative to leaflet attachments.
(B)
Imaging planes and leaflet attachments from (A) shown superimposed on postmortem specimen.
A-M aorto-mitral;
VA ventriculo-arterial.

according to Piazza N, de Jaegere P, Schultz C, Becker AE, Serruys PW, Anderson RH. Anatomy of the aortic valvar complex and its implications for transcatheter implantation of the aortic valve. Circ Cardiovasc Interv 2008;1: 74–81.

The anatomy of the aortic valve and the aortic root be better visualized multidimensional than in a two-dimensional images.

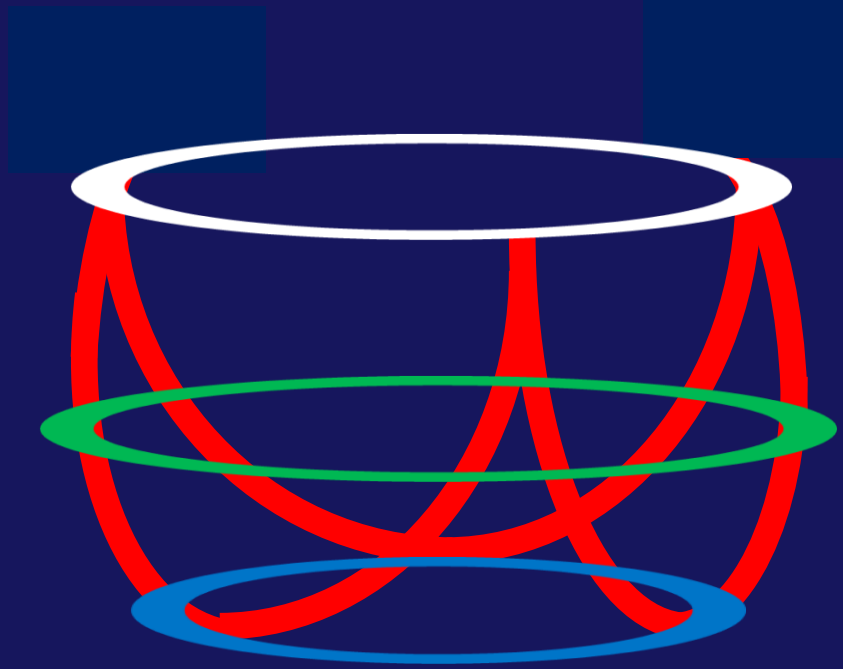

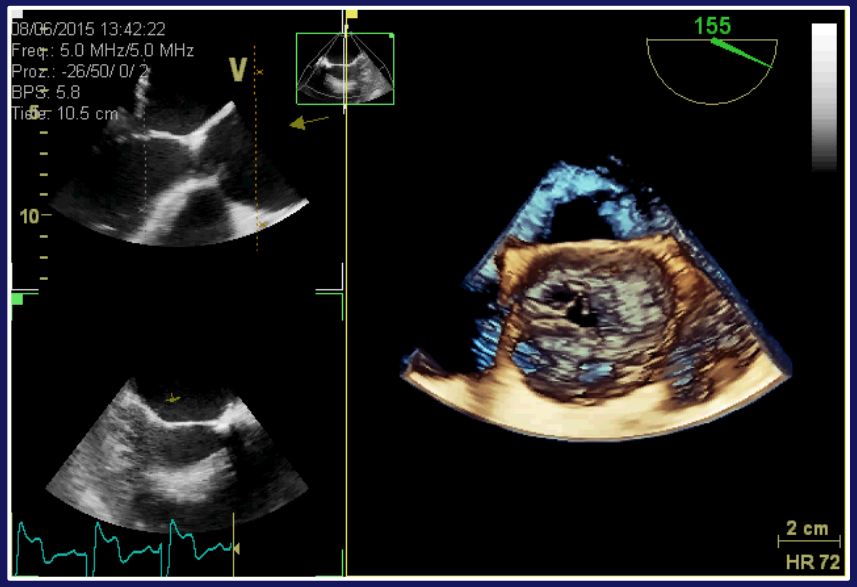

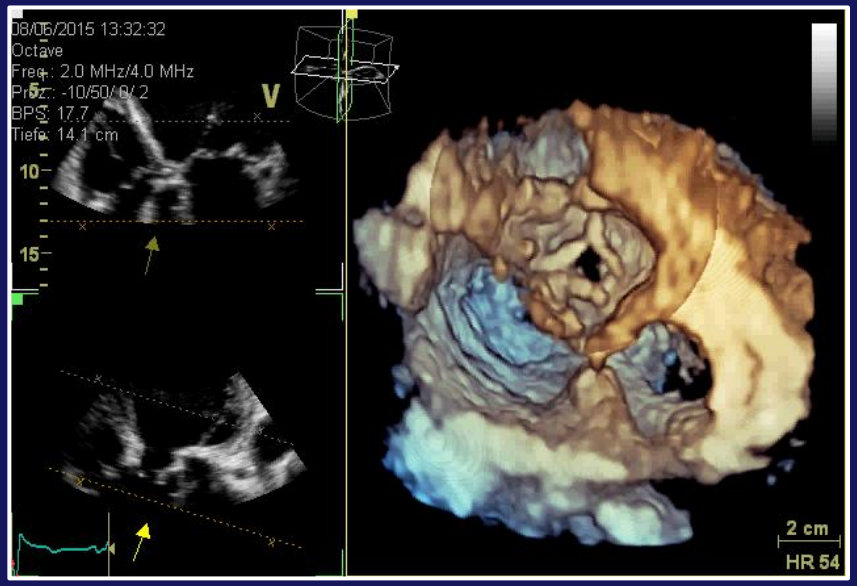

The aortic root: structure, function, and surgical reconstruction

Heart 2000;**83**:376–380

M J Underwood, G El Khoury, D Deronck, D Glineur, R Dion

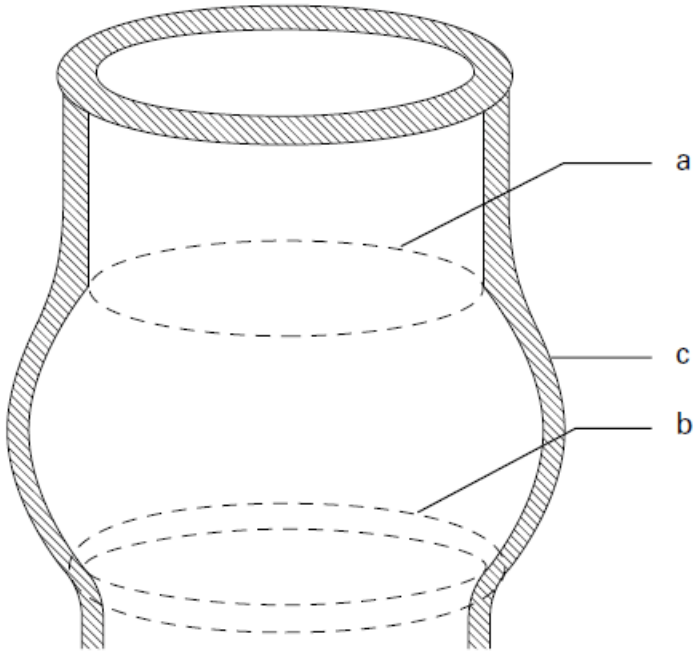

Figure 1 Diagrammatical representation of the aortic root: (a) sinotubular junction; (b) basal ring (surgical annulus); (c) the sinuses of Valsalva.

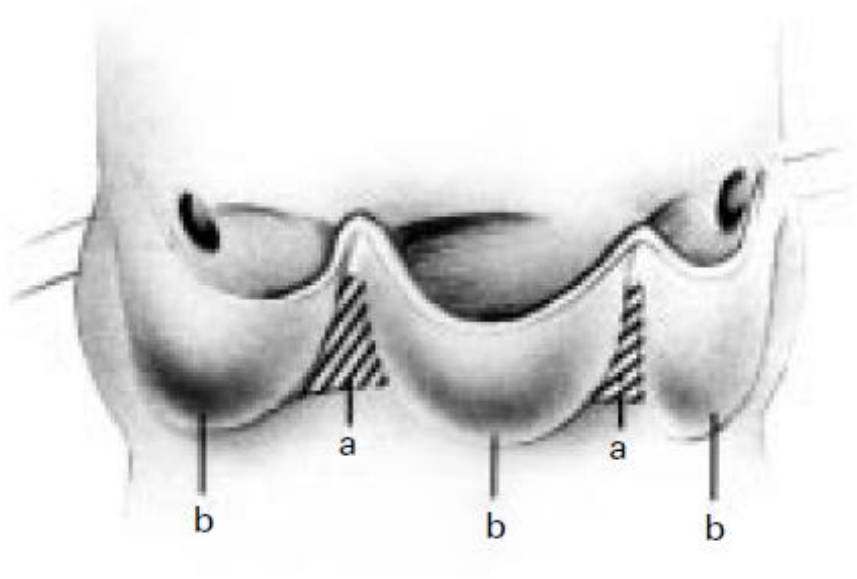

Figure 2 Diagrammatic representation of the aortic root opened longitudinally through the left coronary sinus, demonstrating the interleaflet triangles (a) and the valve leaflets (b).

Transesophageal Echocardiographic Evaluation During Aortic Valve Repair Surgery

(Anesth Analg 2010;111:59–70)

Michel J. Van Dyck, MD,* Christine Watremez, MD,* Munir Boodhwani, MD, MMSc,†
Jean-Louis Vanoverschelde, MD, PhD,‡ and Gebrine El Khoury, MD†

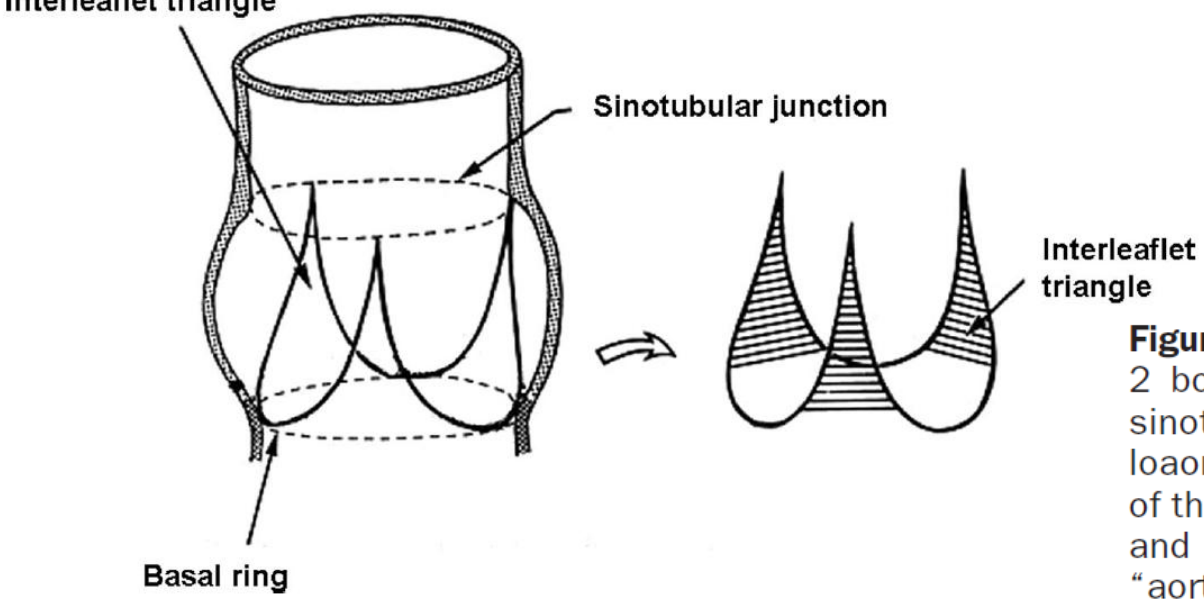

Figure 1. Diagram of the aortic root. The 2 borders of the root are drawn: the sinotubular junction and the ventriculoaortic junction. The basal attachment of the aortic cusps forms the basal ring and is also often described as the "aortic annulus." Inset: The crown-like shape of the valve attachments determines the presence of 3 interleaflet triangles. (Modified from Sutton et al.,[30] with permission.)

according to Van Dyck et al., Anest Analg 2010; 111:59-70

Advanced Course of Reconstruction of the Aortic Valve and Root: A Practical Approach

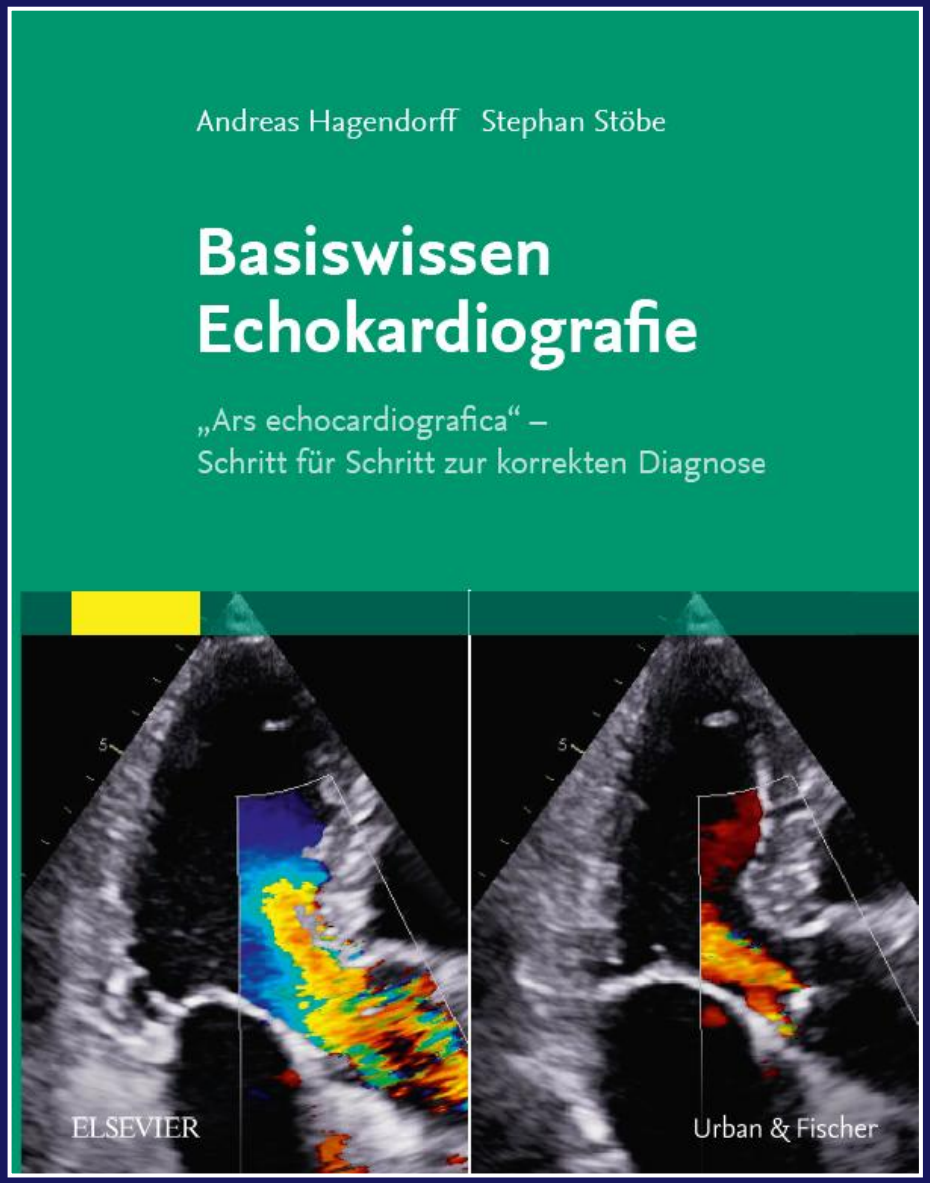

3.3 Die Dokumentation der Herzklappen in der konventionellen Echokardiographie

3.3.1 Die Aortenklappe: Die Darstellung der Aortenklappe in den Standardschnittebenen. Worauf muss bei der exakten Darstellung der Morphologie der Aortenklappe geachtet werden?

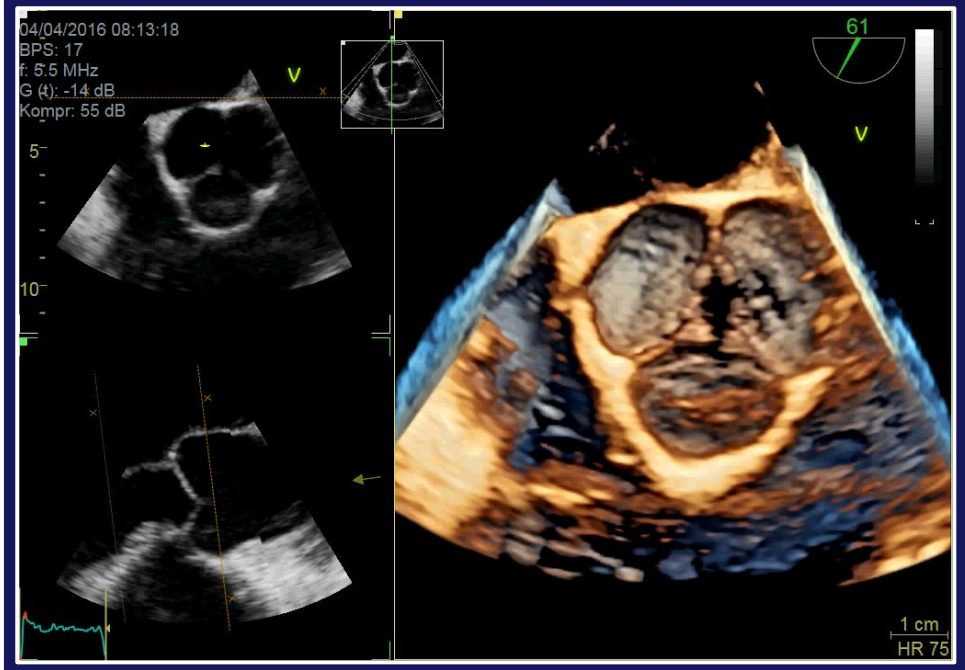

Advanced Course of Reconstruction of the Aortic Valve and Root: A Practical Approach

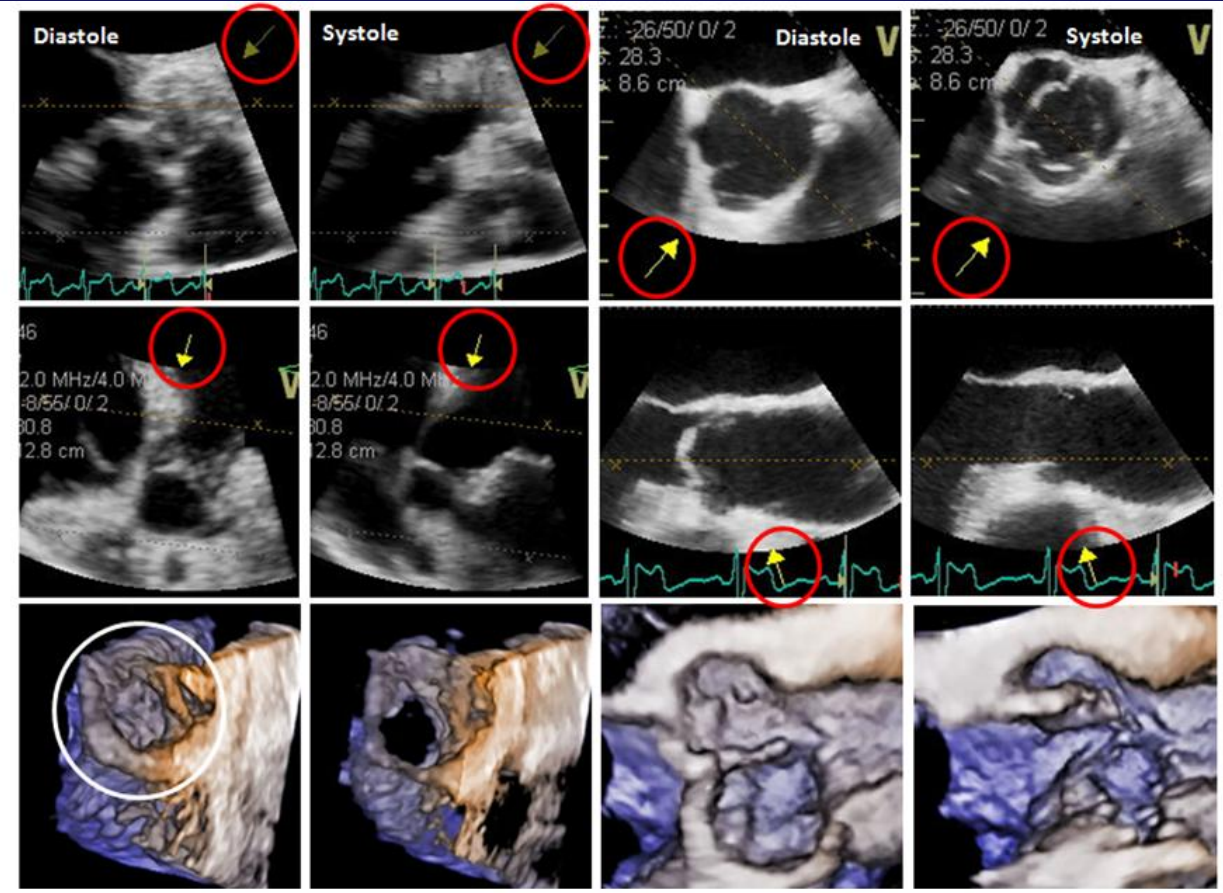

according to
„Basiswissen Echokardiografie“
Hagendorff/ Stöbe 5/2017

Abb. 3.3.6: Multidimensionale Schrägansichten der Aortenklappe zur Darstellung der komplexen Anatomie. In der linken Bildhälfte ist ein ZOOM-Ausschnitt eines transthorakalen 5-Kammerblicks, darunter der zugehörige perpendikuläre Schnitt sowie die multidimensionale Ansicht, die durch die jeweiligen Pfeile in den roten Kreisen gekennzeichnet ist, während der Diastole links und während der Systole rechts dargestellt. In der rechten Bildhälfte ist ein ZOOM-Ausschnitt eines transösophagealen Kurzachsenschnittes der AV, darunter der zugehörige perpendikuläre Schnitt sowie die multidimensionale Ansicht, die durch die jeweiligen Pfeile in den roten Kreisen gekennzeichnet ist, während der Diastole links und während der Systole rechts dargestellt. Links sind gut die „Hinge Points“ der Taschen im "en-face" Blick, rechts in einem Querschnitt zu erkennen.

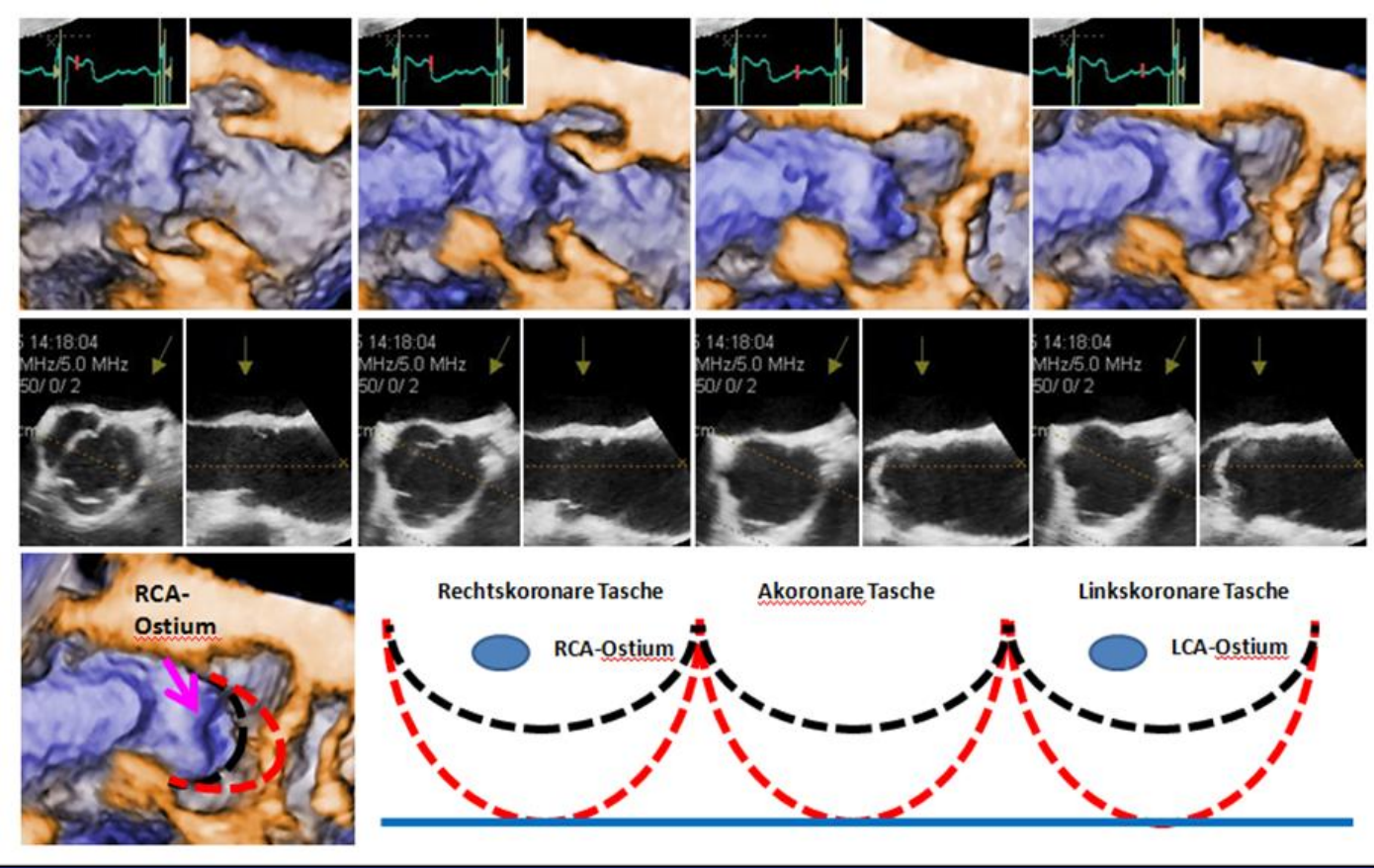

according to „Basiswissen Echokardiografie“ Hagendorff/ Stöbe 5/2017

Abb. 3.3.7: Darstellung der Lage der Koronarostien zu den Taschen der Aortenklappe in der multidimensionalen Echokardiographie. In der oberen Bildreihe sind links zwei Sequenzen während der Systole und rechts zwei Sequenzen während der Diastole abgebildet. Darunter sind die jeweiligen zweidimensionalen biplanen Schnittebenen mit den entsprechenden Blickrichtungen (siehe Pfeile) angeführt. In der unteren Bildreihe ist der Kommissur-bildende Taschenrand in schwarz, der Übergangsbereich zwischen Taschen und Aortenwand in rot sowie das Ostium der rechten Koronararterie mit einem Pfeil im multidimensionalen Bild links beschriftet. Rechts daneben ist eine Schemazeichnung der "aufgeklappten" AV mit Darstellung der Taschenränder abgebildet.

Advanced Course of Reconstruction of the Aortic Valve and Root: A Practical Approach

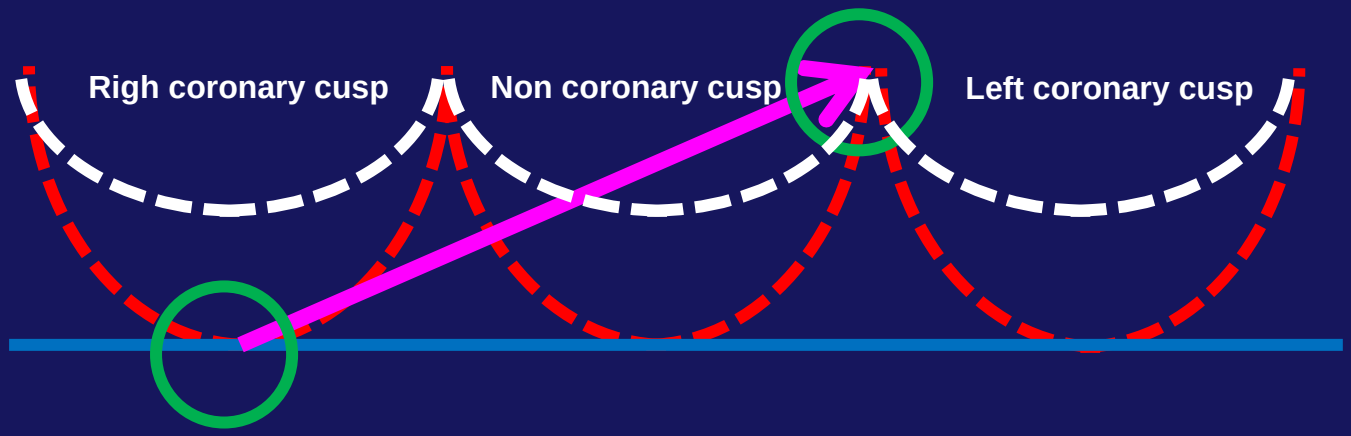

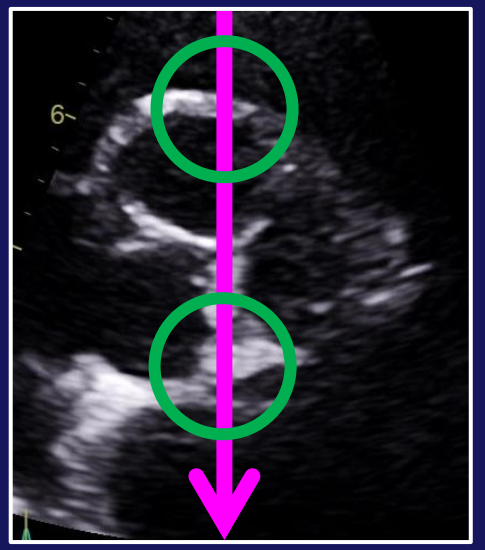

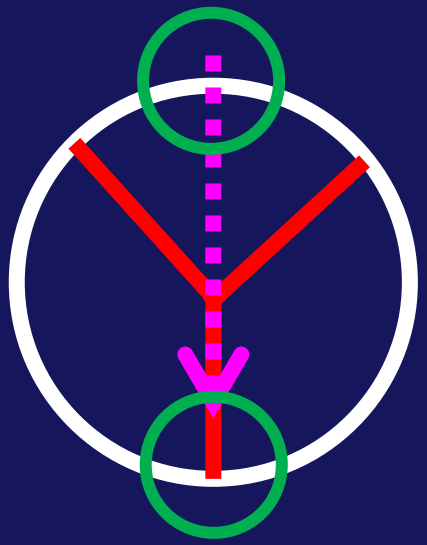

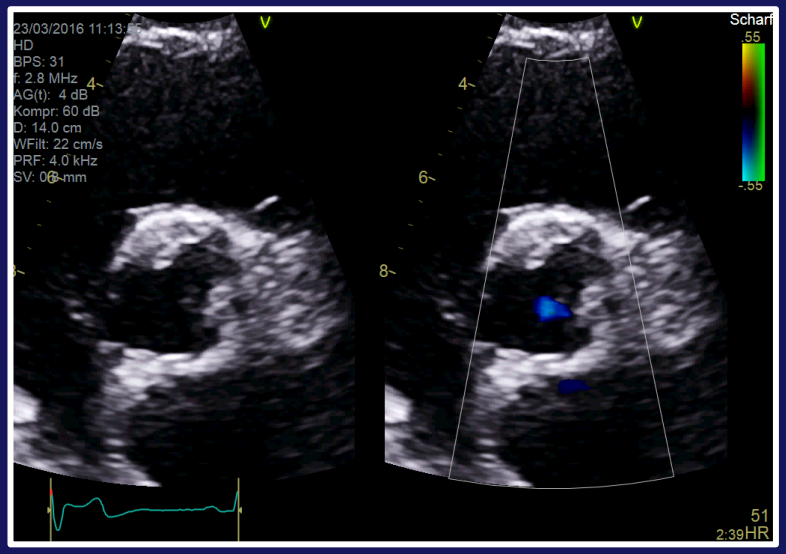

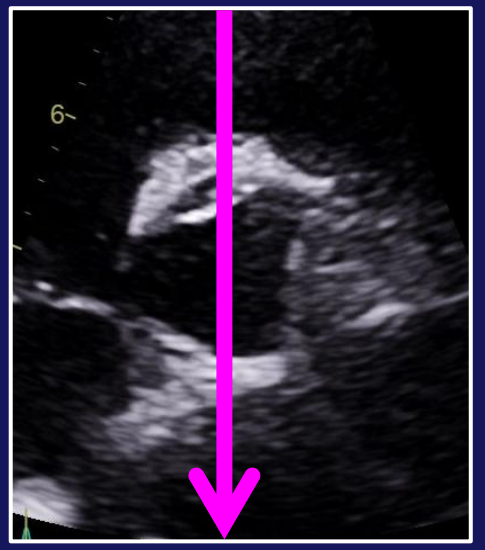

Advanced Course of Reconstruction of the Aortic Valve and Root: A Practical Approach

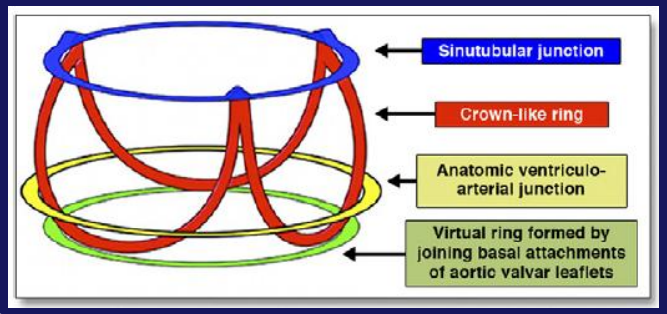

Sinutubular junction

Anatomical ventriculo-arterial junction

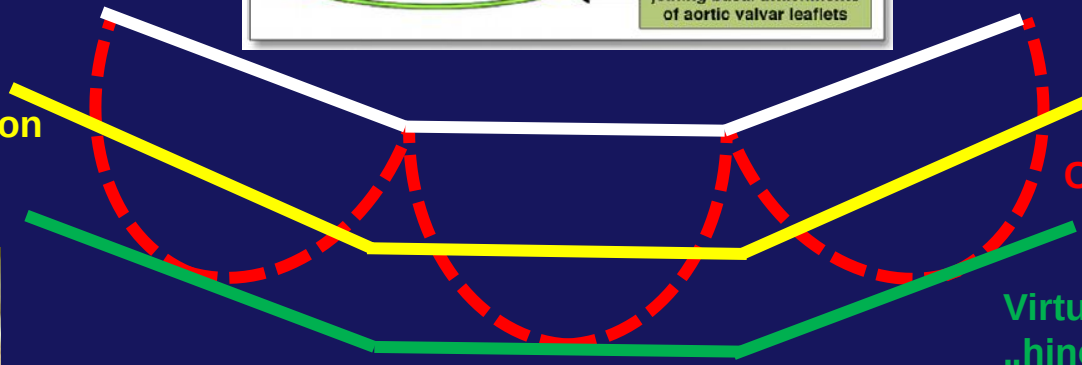

Crown-like ring

Virtual ring formed by the „hinge points“ of the aortic cusps

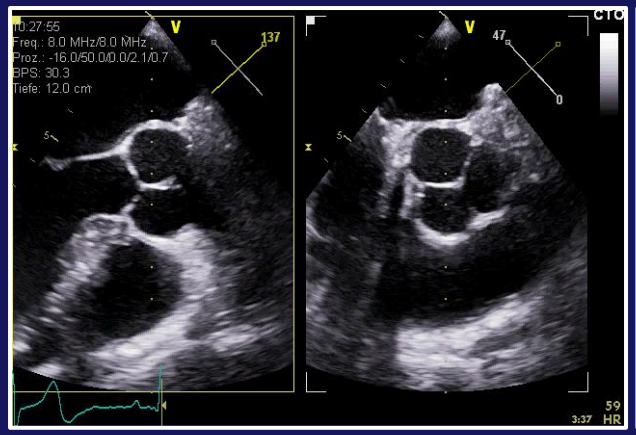

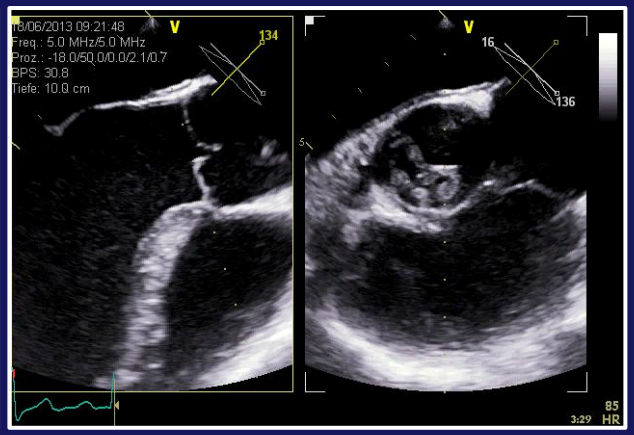

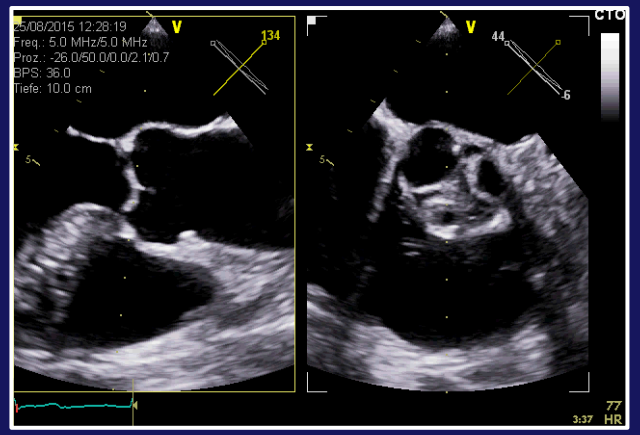

Advanced Course of Reconstruction of the Aortic Valve and Root: A Practical Approach

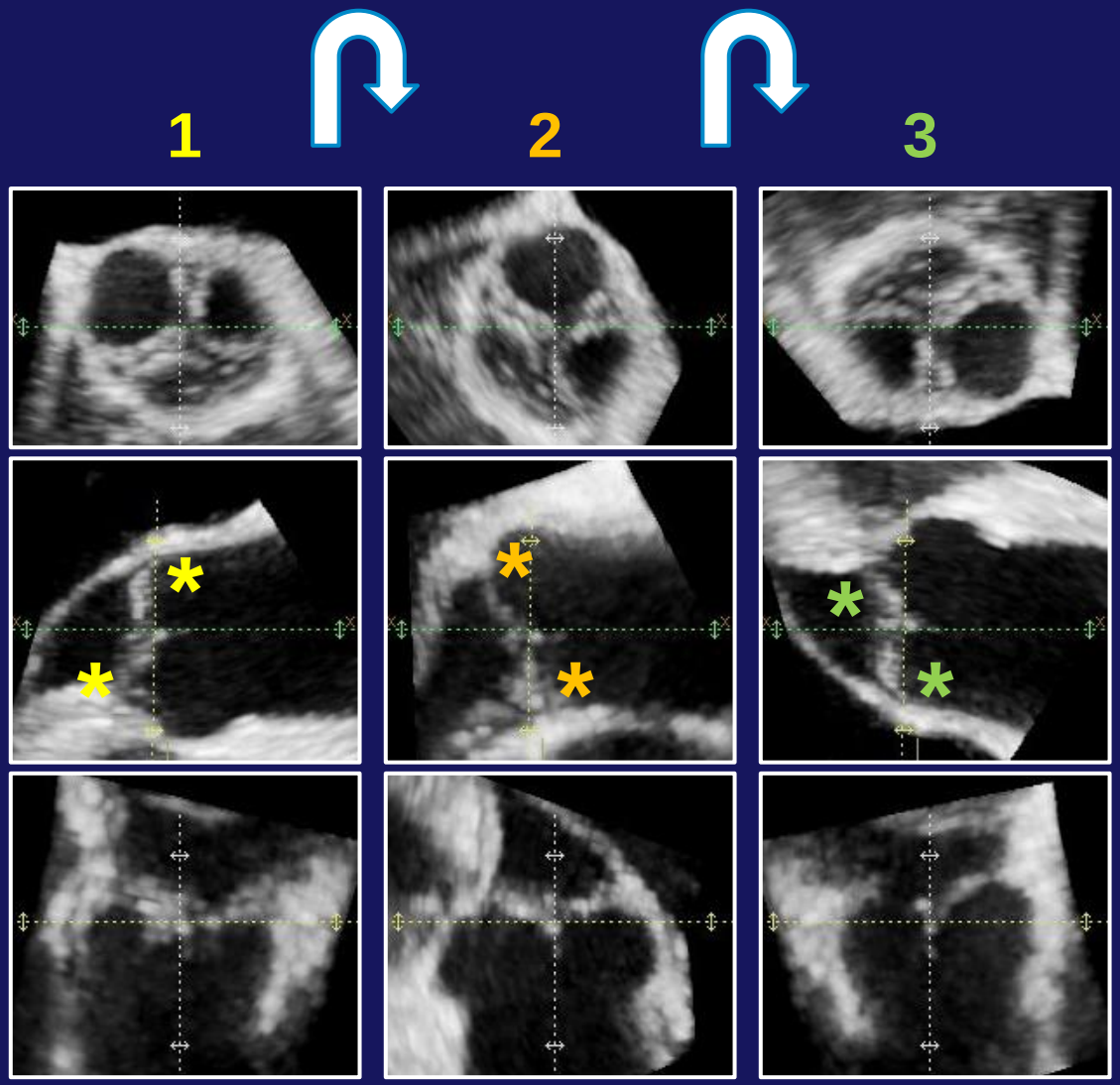

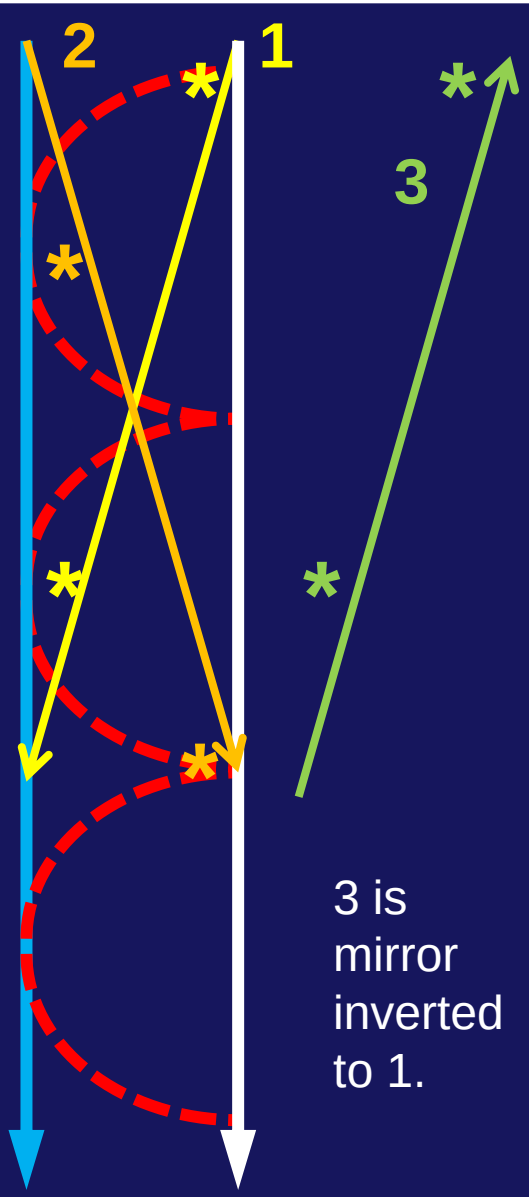

3 is mirror inverted to 1.

Advanced Course of Reconstruction of the Aortic Valve and Root: A Practical Approach

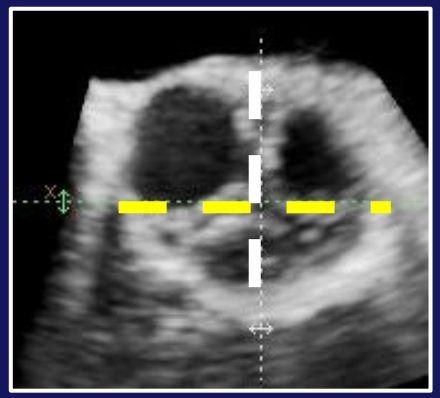

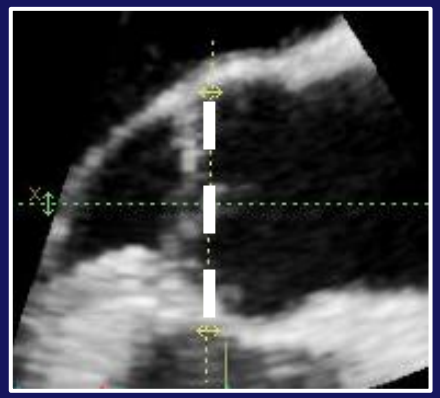

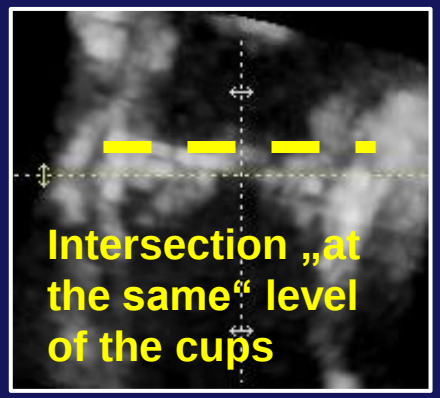

Diastole

Thus,
how to operate correctly?

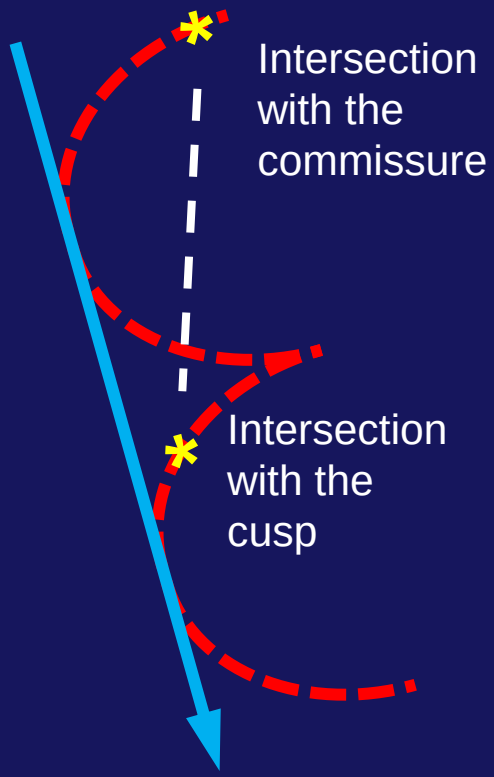

Systole

Intersection with the commissure

Intersection with the cusp

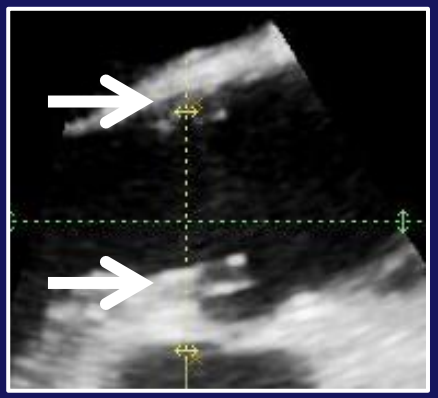

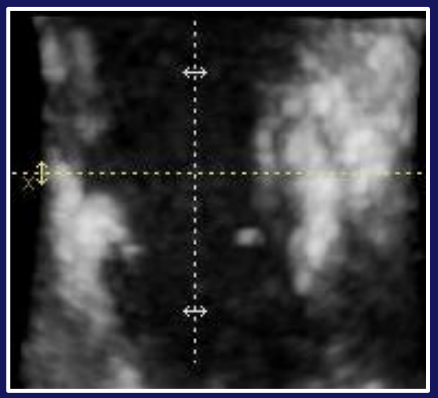

Advanced Course of Reconstruction of the Aortic Valve and Root: A Practical Approach

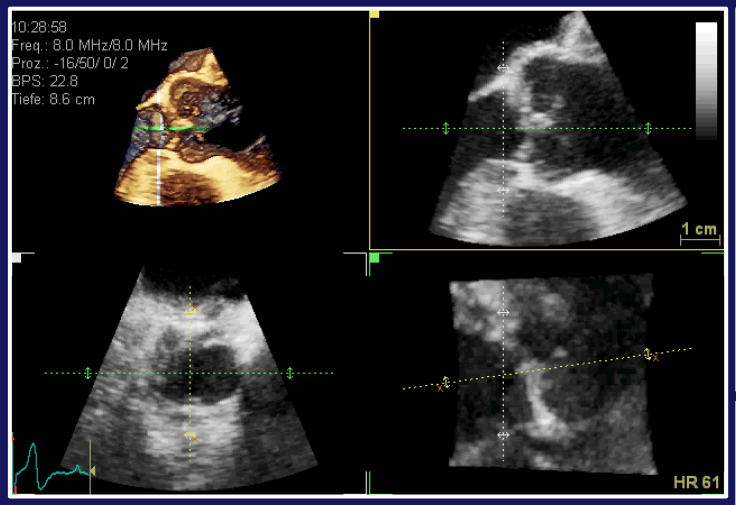

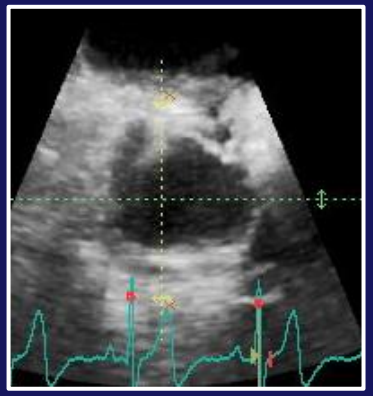

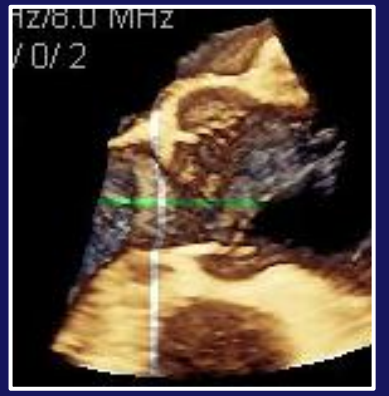

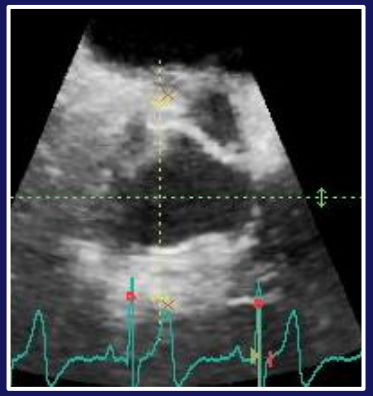

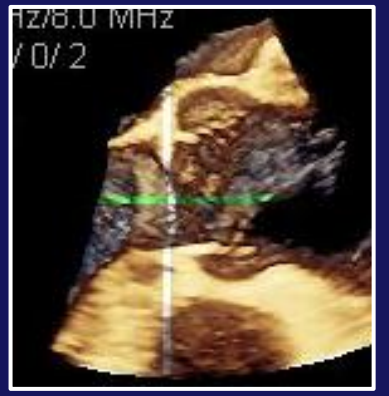

1. step: adjust the central axis of AV during diastole to label the perpendicular plane through the hinge points
2. step: go to systole to measure the widest expansion of the LVOT
3. step: adjust the annulus plane in the LAX view

Advanced Course of Reconstruction of the Aortic Valve and Root: A Practical Approach

aus: J Am Coll Cardiol Img. 2013;6(2):249-262. doi:10.1016/j.jcmg.2012.12.005

Standardized Imaging for Aortic Annular Sizing: Implications for Transcatheter Valve Selection

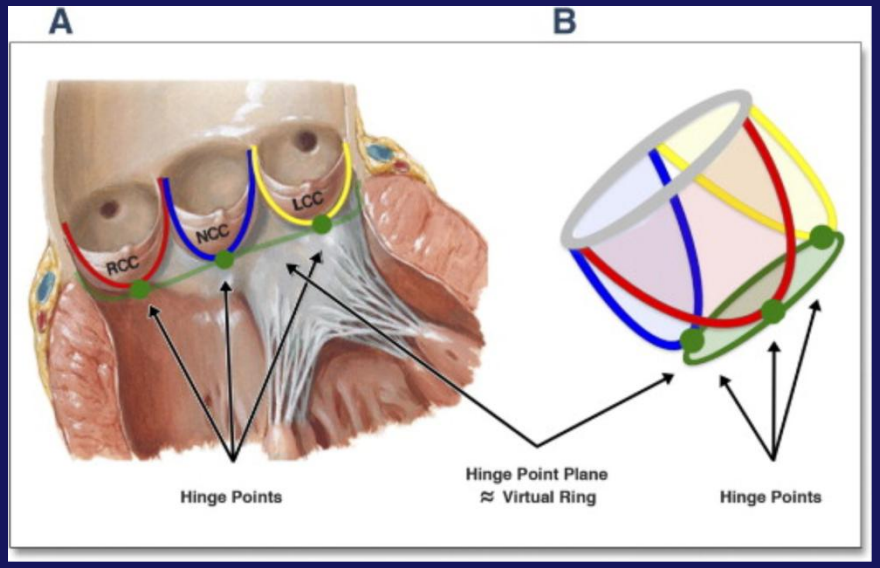

Normal Anatomy of the Aortic Annulus
The aortic annulus accounts for the tightest part of the aortic root (A) and is defined as a virtual ring (green line) with 3 anatomical anchor points at the nadir (green points) of each of the attachments of the 3 aortic leaflets (B). LCC = left coronary cusp; NCC = noncoronary cusp; RCC = right coronary cusp

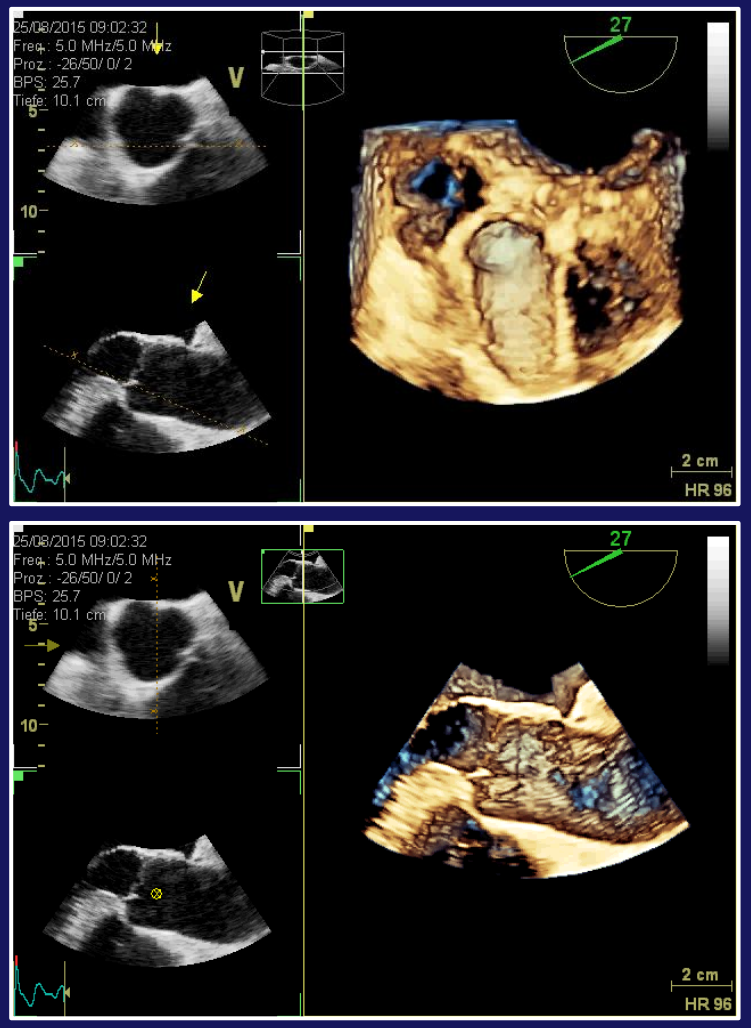

Advanced Course of Reconstruction of the Aortic Valve and Root: A Practical Approach

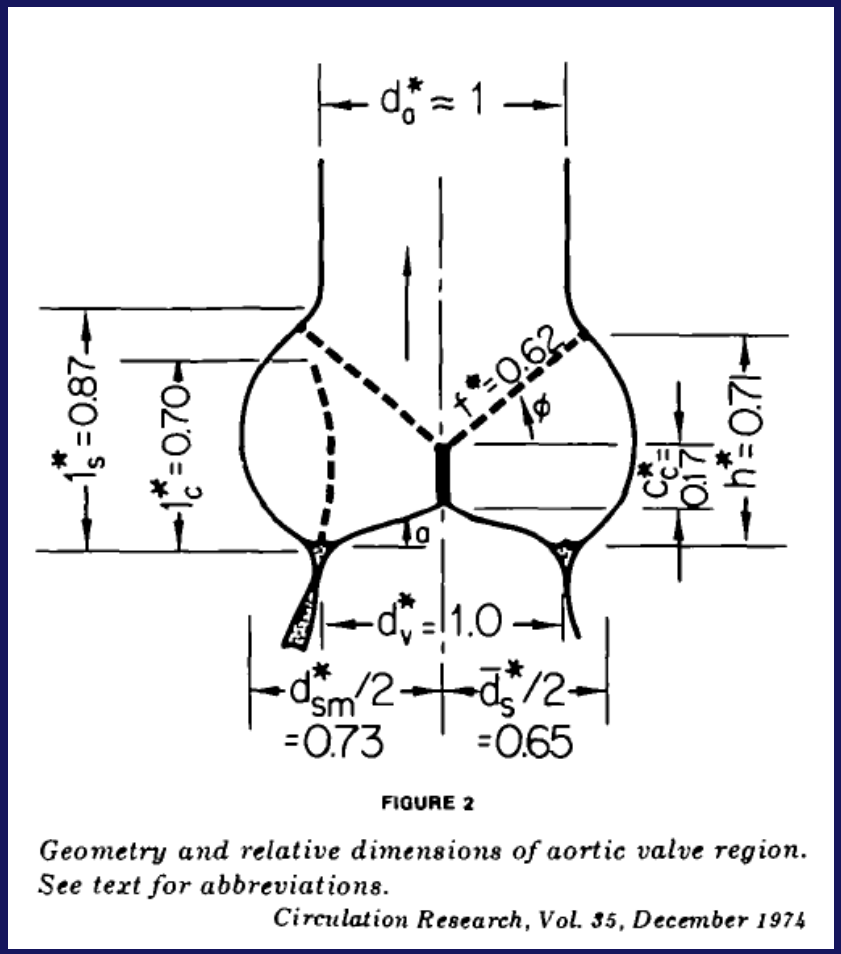

FIGURE 2

Geometry and relative dimensions of aortic valve region. See text for abbreviations.

Circulation Research, Vol. 35, December 1974

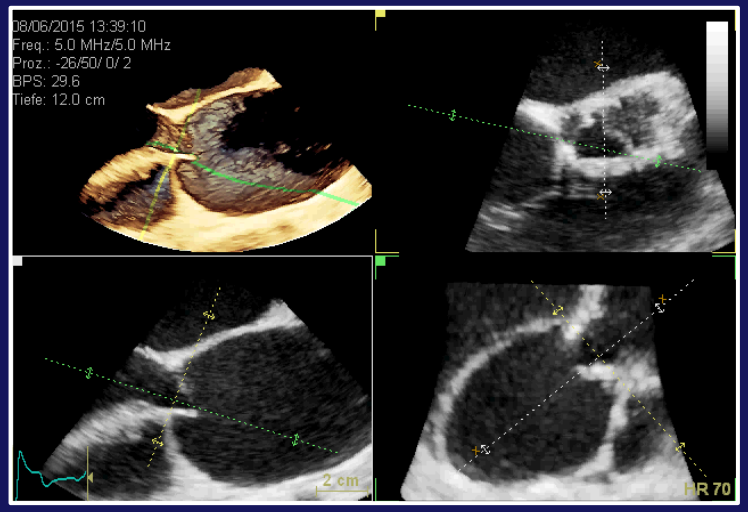

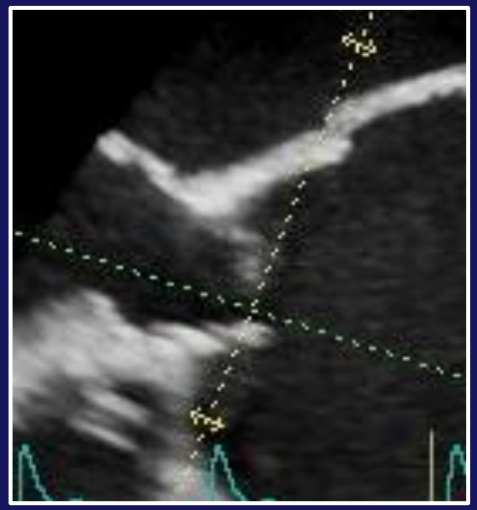

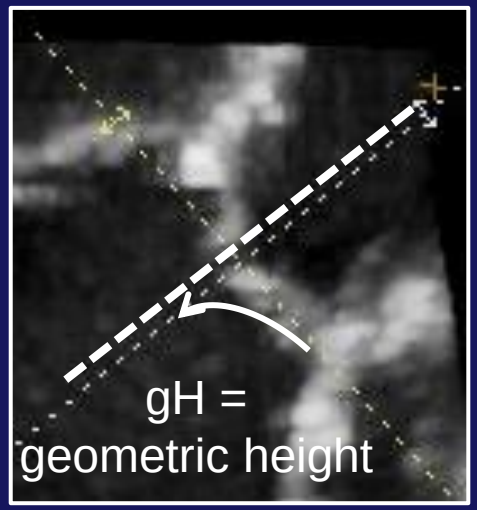

aus Swanson WM and Clark RE. Dimensions and Geometric Relationships of the Human Aortic Valve as a Function of Pressure. Circ Res 1974; 35: 871-882

A Study of Functional Anatomy of Aortic-Mitral Valve Coupling Using 3D Matrix Transesophageal Echocardiography

Federico Veronesi, PhD; Cristiana Corsi, PhD; Lissa Sugeng, MD, MPH; Victor Mor-Avi, PhD; Enrico G. Caiani, PhD; Lynn Weinert, BS; Claudio Lamberti, MS; Roberto M. Lang, MD

Conclusions—This is the first study to report quantitative 3D assessment of the mitral and aortic valve dynamics from matri array transesophageal images and describe the mitral-aortic coupling in a beating human heart. This ability may have impac on patient evaluation for valvular surgical interventions and prosthesis design. (***Circ Cardiovasc Imaging*. 2009;2:24-31.**)

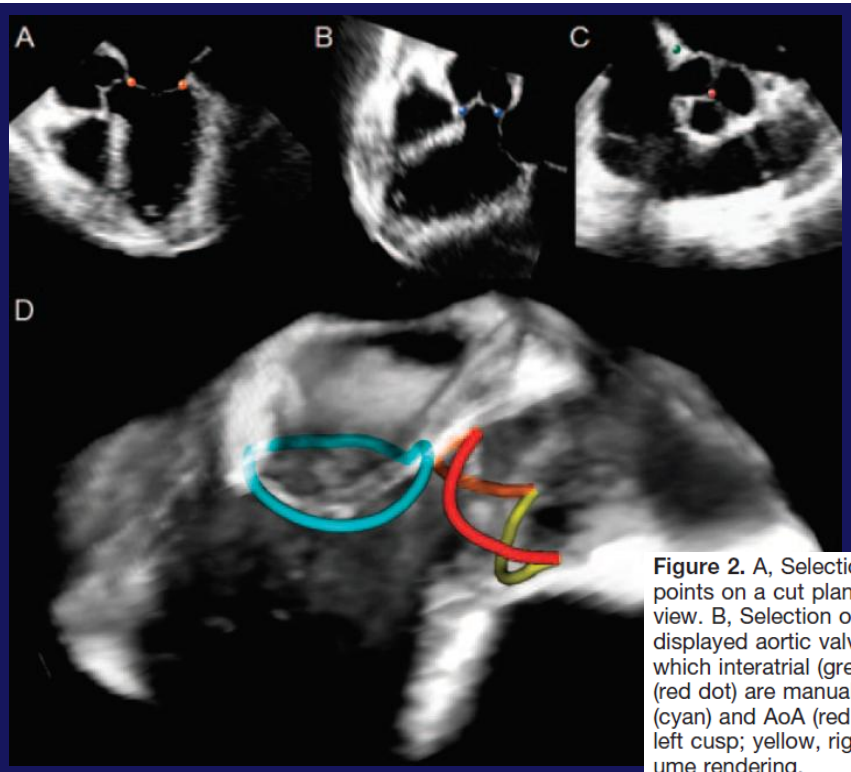

Figure 2. A, Selection of anterior and posterior MA points on a cut plane representing 3-chamber view. B, Selection of AoA points. C, Automatically displayed aortic valve short axis cut plane on which interatrial (green dot) and coaptation point (red dot) are manually identified. D, Computed MA (cyan) and AoA (red, noncoronary cusp; orange, left cusp; yellow, right cusp) splines on RT3DE volume rendering.

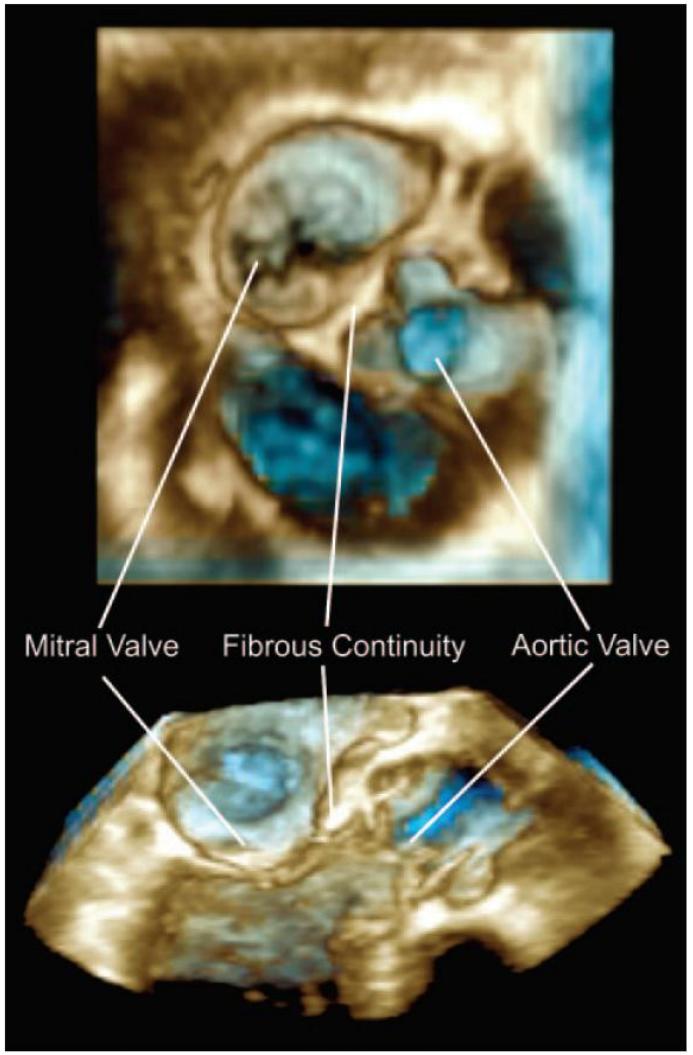

Figure 1. Volume rendering of RT3DE mTEE data visualized from atrium (top) and in a long axis view (bottom).

Advanced Course of Reconstruction of the Aortic Valve and Root: A Practical Approach

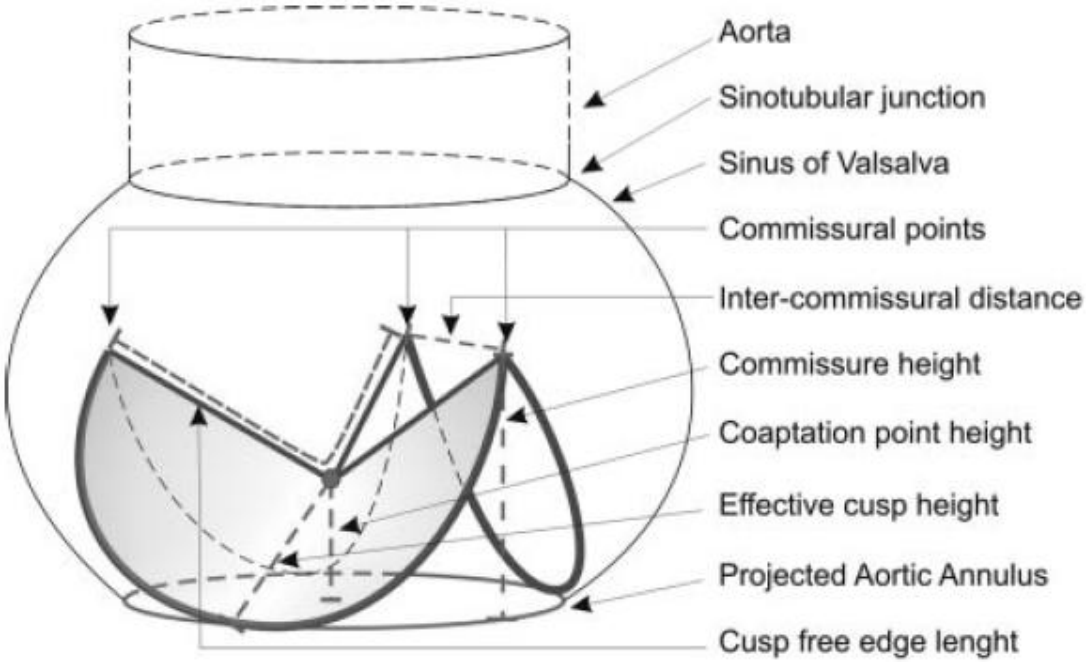

Figure 3. Schematic of automatically extracted AoA measurements.

Figure 5. Left, Mitral and aortic annuli computed from a RT3DE data set obtained in a patient with severe sclerocalcific aortic stenosis, shown superimposed on a 3-chamber view. Note that the angle between the 2 valves is severely reduced (93°) compared with normal subjects and also the distance between the 2 valve was just 18 mm and did not changed during cardiac cycle. The aortic stenosis was most likely responsible for the reduced change in projected AoA area during the cardiac cycle, having a negative impact on the aortic-mitral coupling as reflected by a decrease in maximum diastolic area change to only 12%, compared with 25.4% of the ED area in normal subjects (Table 1). Right, Mitral and aortic annuli computed from a RT3DE data set obtained in a patient with implanted mitral ring, shown superimposed on a 2-chamber view. Note the deformation in the shape of the AoA. In this subject, reduced motion of the mitral valve (4.5 mm maximum at ES) and reduced MA height (4.3 mm) at ED was noted. In addition, the intercommissural distances where asymmetrical: the distance between the commissures of the left cusp was smaller (18 mm) compared with the noncoronary and right cusps (28 and 27 mm, respectively). Moreover, the saddle shape of the MA was not preserved because of the rigid ring.

Advanced Course of Reconstruction of the Aortic Valve and Root: A Practical Approach

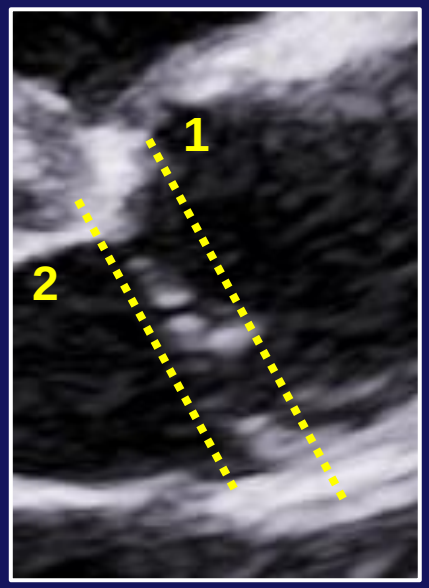

1=
diameter at the level of the tpis of the „crown-like“ ring

2=
diameter at the level of the „hinge points“

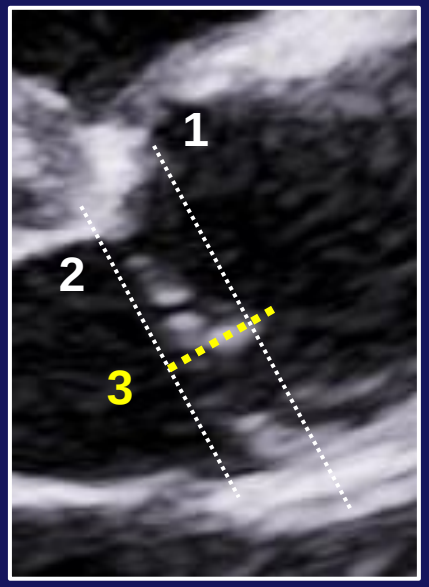

3 =
effective height

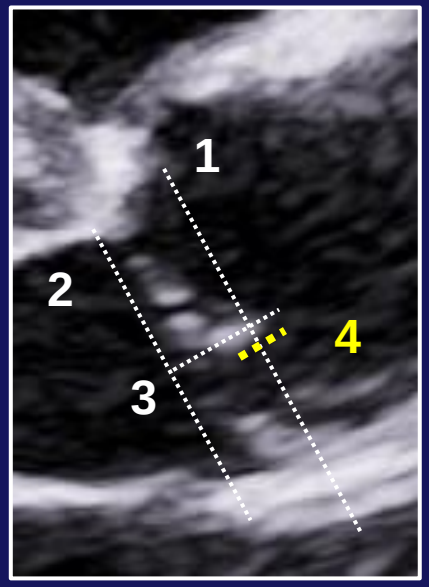

4 =
coaptation-length

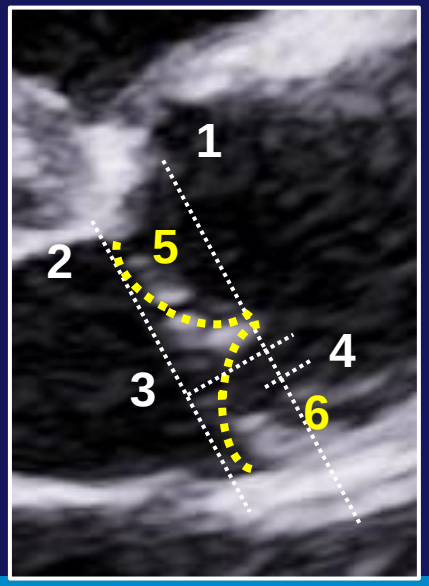

5 and 6 =
geometric heights of the cusps
- Really visualized only for the right coronary cusp

Advanced Course of Reconstruction of the Aortic Valve and Root: A Practical Approach

Steps for measurement of geometric and effective height

1

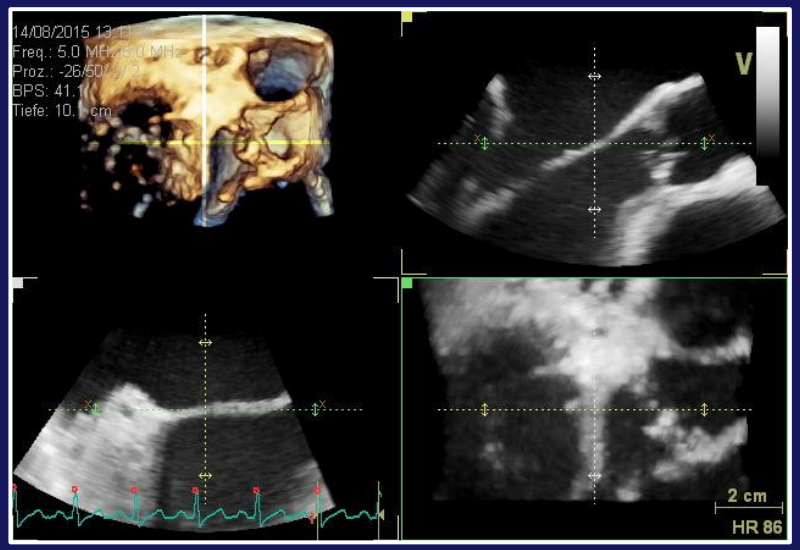

2

3

1. Acquire a ZOOM data set of the complete mitral and aortic valve
2. Adjust the central axis of the aortic root in the long axis (systole/diastole)
3. Adjust the central axis of the aortic root in the perpendicular axis
4. Adjust the short axis to the hindge points by translation during diastole
5. Rotate the short axis view to control the sectional short axis plane..

Advanced Course of Reconstruction of the Aortic Valve and Root: A Practical Approach

Von: jimg@msubmit.net [mailto:jimg@msubmit.net]
Gesendet: Donnerstag, 21. Juni 2018 16:02
An: Hagendorff, Andreas
Betreff: JIMG021818-0232R1 Decision Letter

"Improvement in the Assessment of Aortic Valve and Aortic Aneurysm Repair by 3D-Echocardiography"

Dear Prof. Hagendorff:

On behalf of the American College of Cardiology, we are pleased to accept your above referenced manuscript for publication.

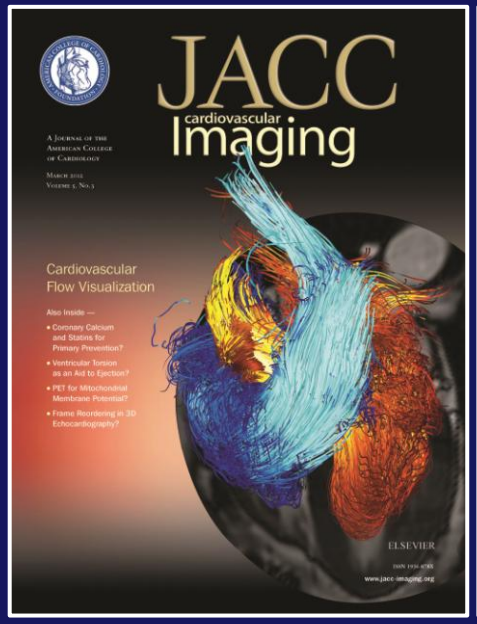

Improvement in the Assessment of Aortic Valve and Aortic Aneurysm Repair by 3D-Echocardiography

Andreas Hagendorff[1], Arturo Evangelista[2], Wolfgang Fehske[3], Hans-Joachim Schäfers[4]

[1] Department of Cardiology, University of Leipzig, Leipzig, Germany;
[2] Servei de Cardiologia. Hospital Universitari Vall d´Hebron. CIBER-CV. Barcelona, Spain;
[3] Innere Medizin III-Kardiologie, St. Vinzenz Hospital, Cologne, Germany;
[4] Department of Thoracic and Cardiovascular Surgery, Saarland University Medical Center, Homburg/Saar, Germany

Short title: 3D- Echocardiography in Aortic Valve Repair
Word count: 6141

Abstract:
Reconstructive surgery of the aortic valve repair has become increasingly employed in patients with aortic regurgitation and/or aortic aneurysm. Its success depends on restoring normal aortic valve and root form. Echocardiography is the most reliable and precise imaging technique since it defines abnormal morphology and function, essential for selecting appropriate substrates and guiding the surgical strategy.
This review focuses on the use of 3D-echocardiography to characterize different forms of aortic valve and root abnormalities and attempts to define echocardiographic predictors of successful valve/root complex repair.

in press – JACC Imaging 2018

Advanced Course of Reconstruction of the Aortic Valve and Root: A Practical Approach

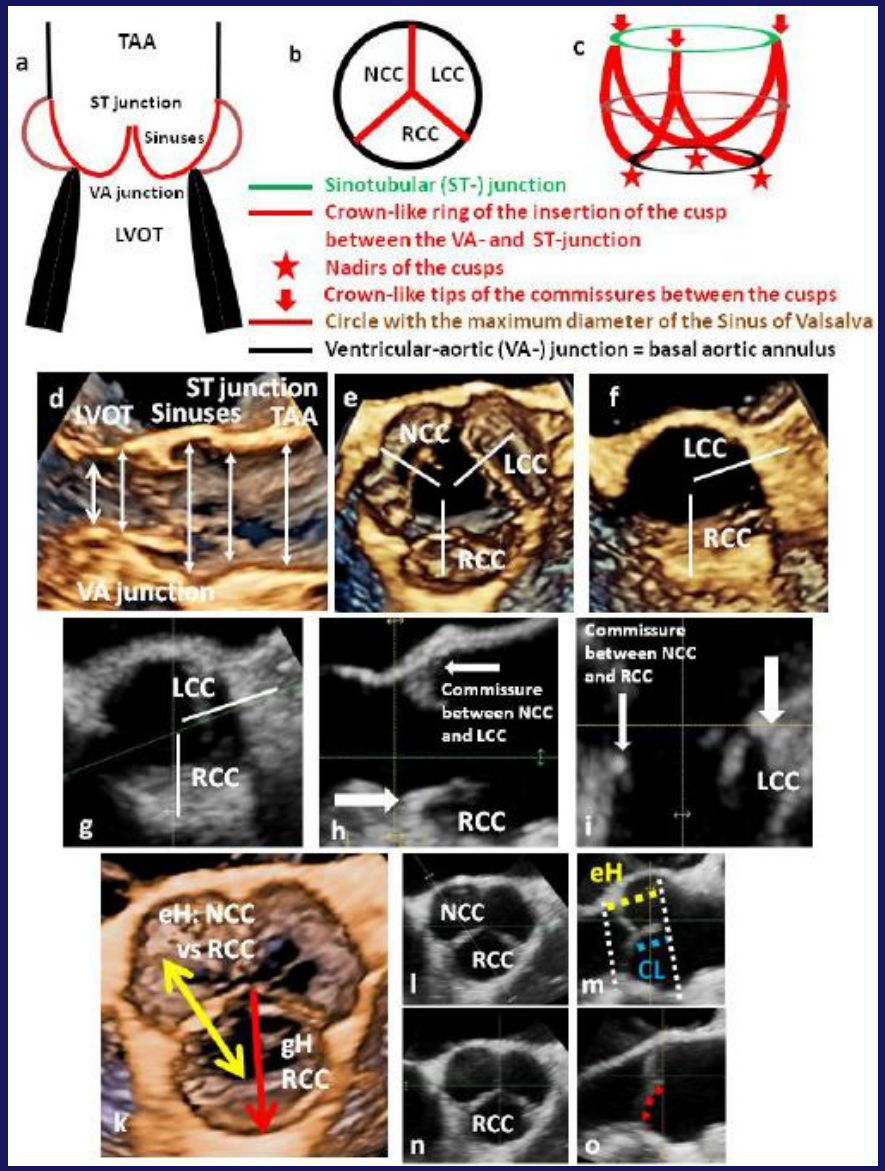

Central Illustration: The figure summarizes the advantages of applying the 3D technique to the analysis of aortic valve and aortic root complex prior to surgical correction. Sketches of the aortic valve (AV) and aortic root (long-axis view: a, short-axis view: b, 3D view: c). Parameters such as diameter of the ventricular-aortic (VA)-junction, aortic root and sinotubular (ST)-junction as well as effective height (eH) and geometric height (gH) of each cusp can be more objectively and accurately assessed by 3D echocardiography versus 2D echocardiography. Labeling of the essential parameters in 3D long-axis view (d), 3D short-axis view of the AV (e) and VA junction (f). Exemplary illustration of the adjustment of the correct sectional plane of the VA junction (g-i). Exemplary illustration of the adjustment of eH (yellow) and coaptation length (CL) (blue) between non- (NCC) and right coronary cusp (RCC) and of gH (red) of the RCC.

according
Hagendorff et al. J Am Coll Cardiol Img 2018; in press

Advanced Course of Reconstruction of the Aortic Valve and Root: A Practical Approach

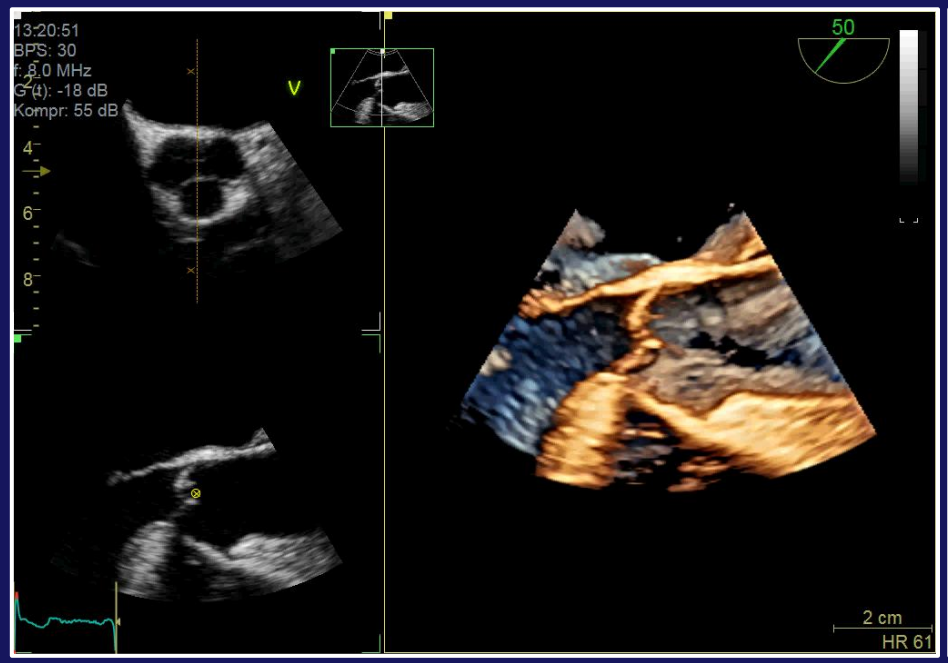

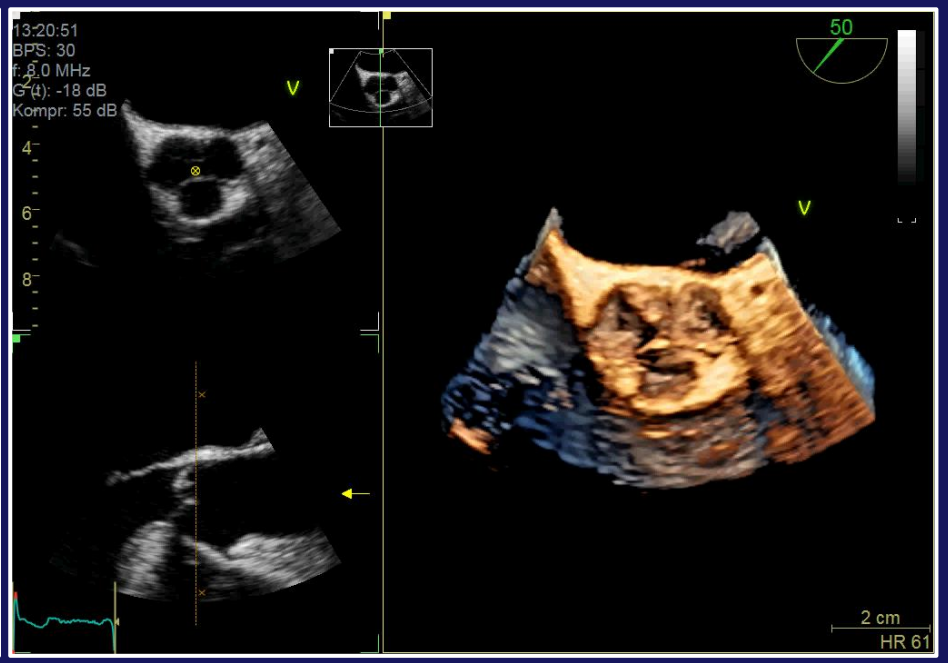

To analyze the aortic valve and the aortic root the main prerequisite is to acquire 3D-image data sets with optimal image quality and the best possible temporal and spatial resolution.
Optimization of ultrasound settings in 2 D an 3D is extremely important

Advanced Course of Reconstruction of the Aortic Valve and Root: A Practical Approach

Prerquisite for excellent image quality
in 2D as well as 3D echocardiography:
knowledge about ultrasound physics and implementation of these aspects into the workflow by just technical knowledge about the buttons.
and in case of interventions and surgery – training for a fast workflow.

Then, detailed information about aortic valve and aortic root morphology is possible.
The spatial and temporal resolution of 3D TEE is at least comparable to cardiac-CT.

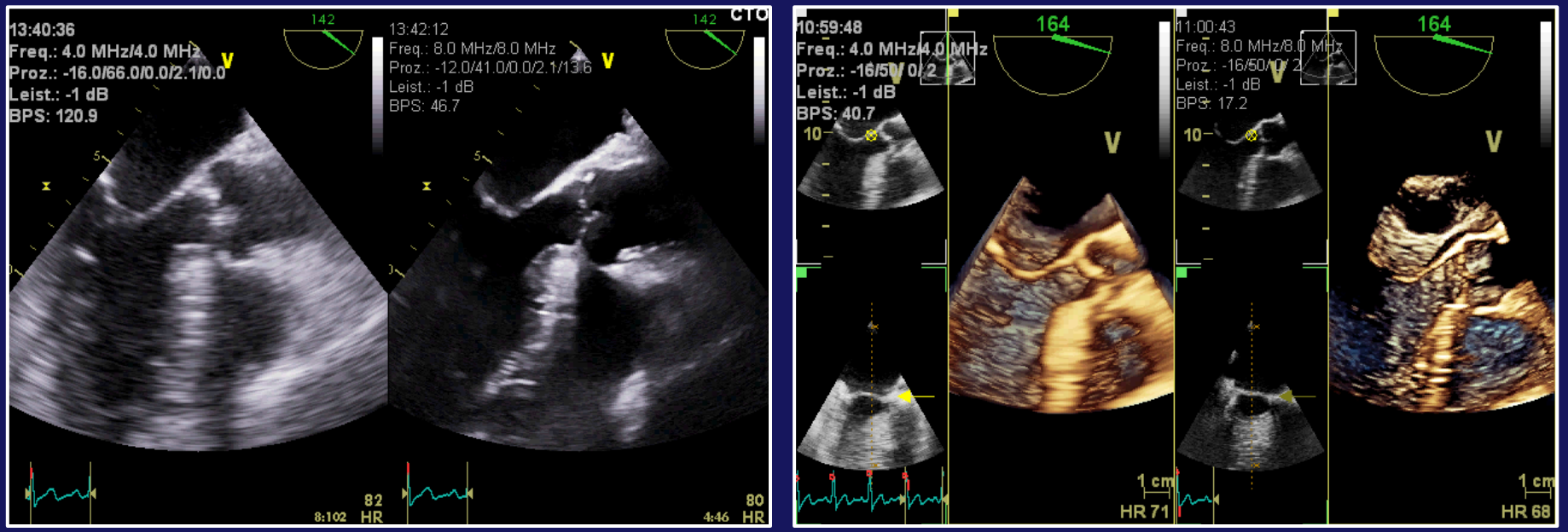

The same patients: „bad“ settings versus optimized settings in 2D and 3D-TEE.

Advanced Course of Reconstruction of the Aortic Valve and Root: A Practical Approach

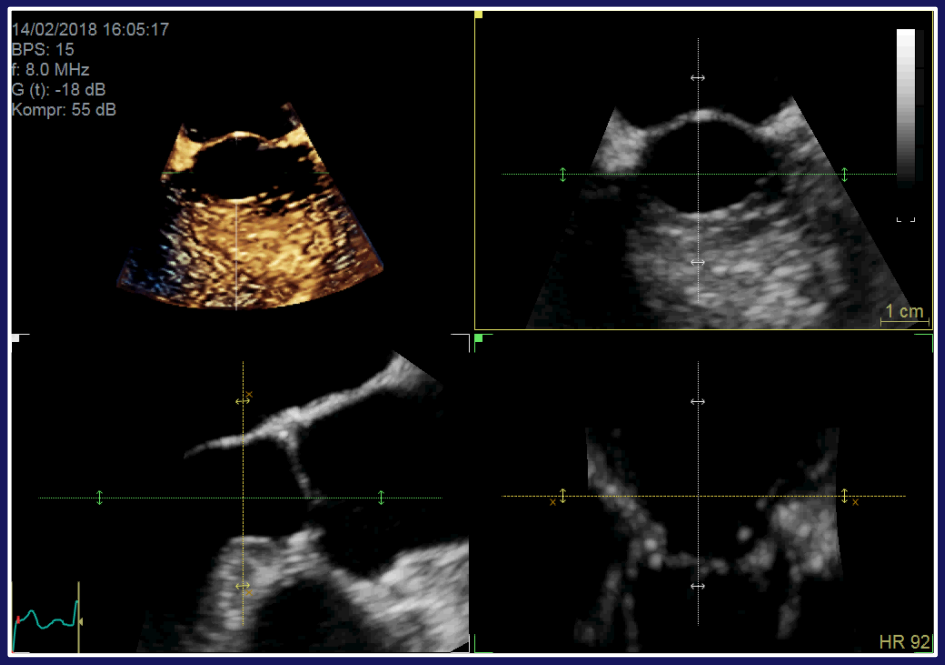

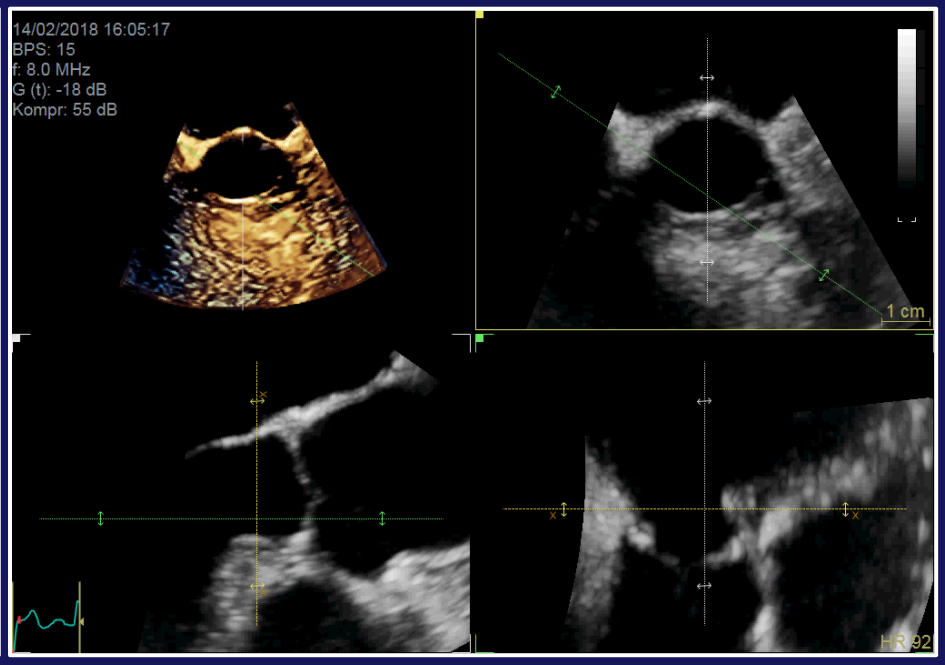

LVOT

Sinuses

ST-junction

TAA

VA-junction

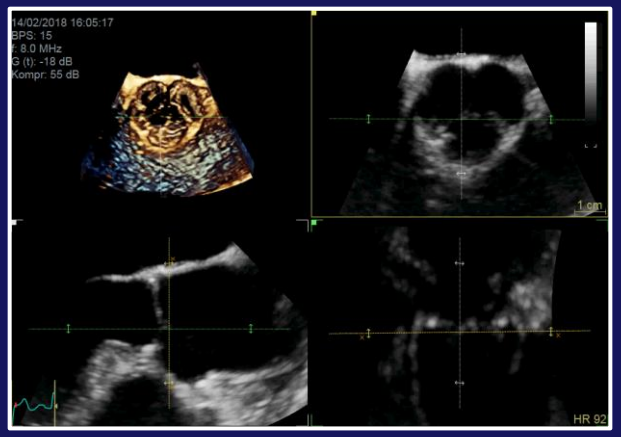

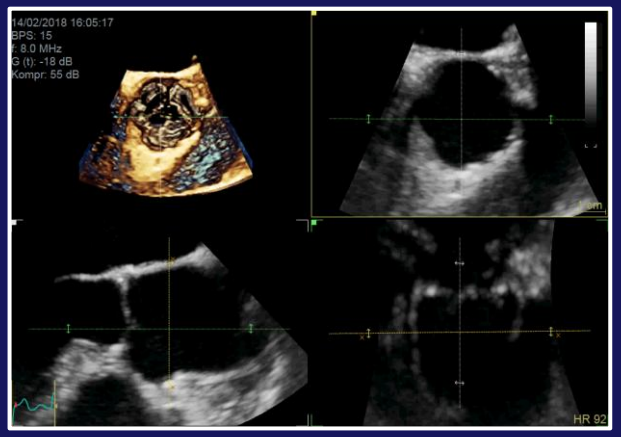

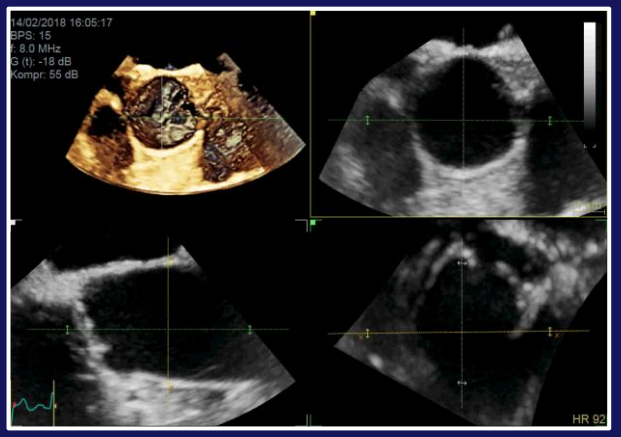

Advanced Course of Reconstruction of the Aortic Valve and Root: A Practical Approach

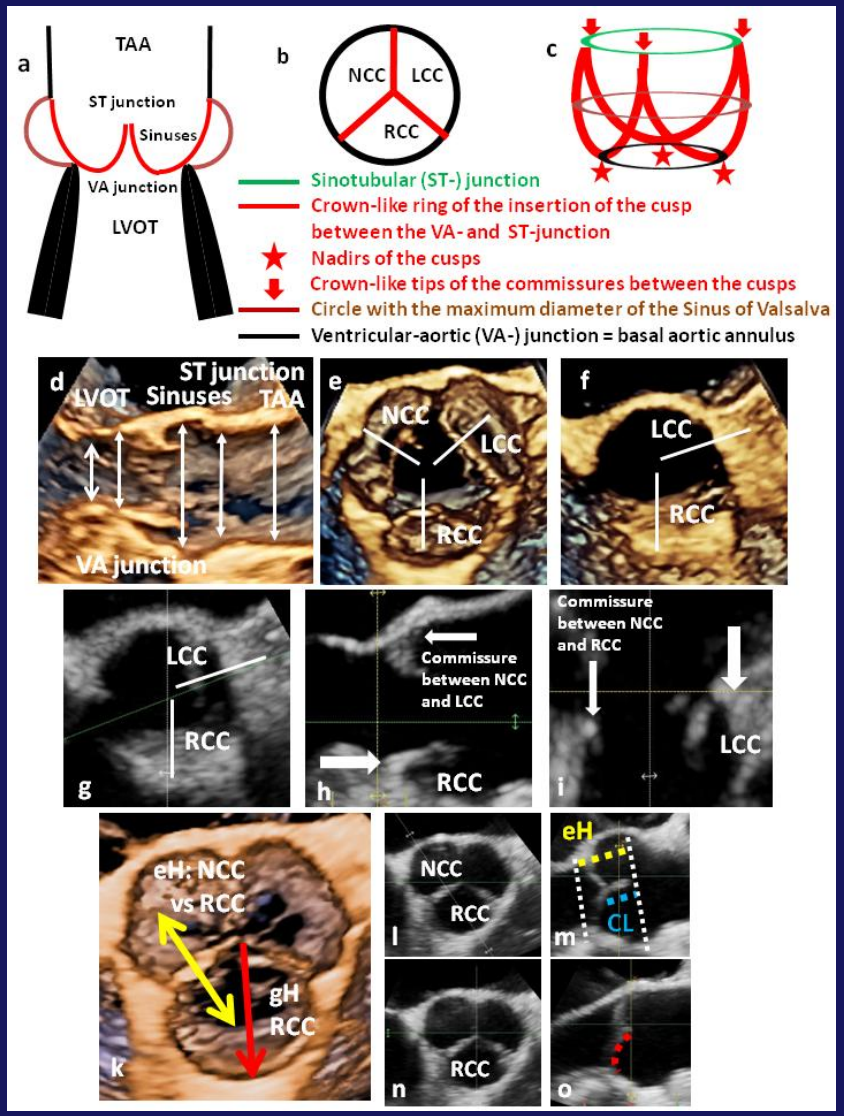

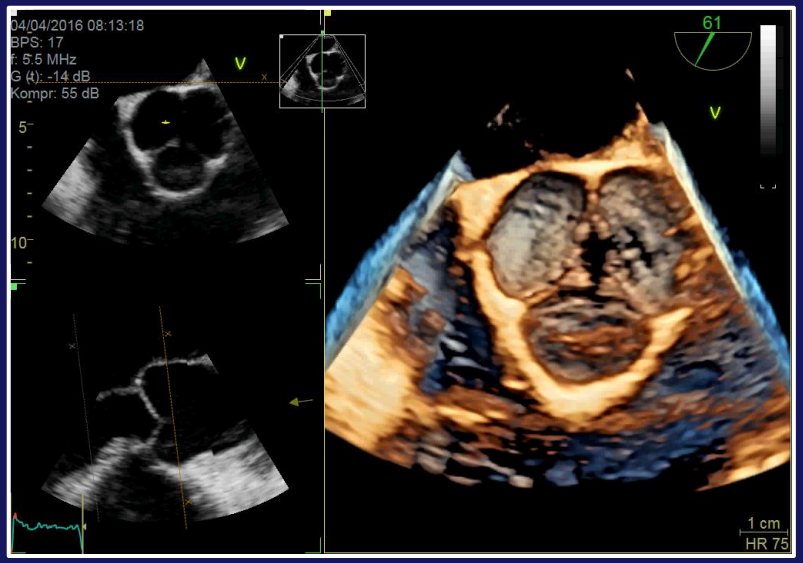

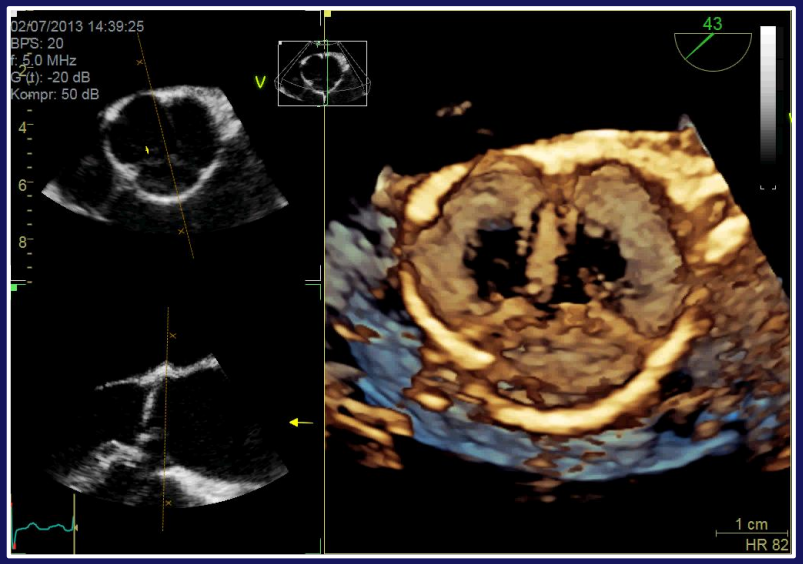

according Hagendorff et al. J Am Coll Cardiol Img 2018; in press

Final recommendations according to the authors` experience and literature (1)

The results of echocardiographic measurements of the AV and aortic root strongly depend on the time point of the cardiac cycle. The maximum anterior-posterior diameter of the LVOT, AV annulus, SV, ST junction and TAA obviously vary between systole and diastole. These dimensions are larger during systole than diastole, especially in younger patients with preserved compliance of the aortic root. These dimensions are important for decision making in AV reconstruction, which is generally performed in younger patients. Given these considerations, we strongly feel that the AV complex measurements should be performed in mid-systole.

according Hagendorff et al. J Am Coll Cardiol Img 2018; in press

Final recommendations according to the authors` experience and literature (2)

…..

In addition, spatial resolution of the external aortic wall using 3D TTE and 3D TEE may be limited. Owing superior demarcation of the inner aortic wall – especially using 3D TEE – we believe that I-I measurements are superior to L-L measurements when using 3D echocardiography. Finally, underestimation is unavoidable in 2D TEE for the reasons stated. Thus, correct determination of these important diameters can best be achieved by I-I measurements during mid-systole using standardized sectional planes within the 3D data sets by postprocessing. This creates a contradiction regarding proposed mid-systolic measurements and current guideline recommendations. Current guidelines, however, do not address the specific aspects of AV repair. Furthermore, several studies showed that using I-I convention underestimation was compensated for by measuring aortic diameters mid-end-systole.

according Hagendorff et al. J Am Coll Cardiol Img 2018; in press

Final recommendations according to the authors` experience and literature (3)

…..

Measurements of cusp morphology and geometry – especially CL, eH and gH – obviously have to be performed during diastole when the cusps are stretched by diastolic pressure. All findings and parameters for the assessment of the AV root complex which are relevant and mandatory according to our experience, are highlighted in Table 1.

according Hagendorff et al. J Am Coll Cardiol Img 2018; in press

Summary

3D Echocardiography is the best imaging technique for patient selection for surgical AV repair and AV-sparing surgery. 2D-TTE and 2D-TEE are inferior to 3D-echocardiography owing to misleading measurements in non-standardized, oblique sectional planes. 3D echocardiography should include analysis of AV morphology, aortic root dimensions and AR severity. Cusp morphology and commissures and measurements of coaptation length, eH and gH parameters should be described in a systematic approach using mainly 3D TTE and 3D TEE. Complete and concise analysis by 3D echocardiography enables correct decision-making and planning of surgical procedures in patients with AR and aortic valve/root abnormalities. It can be assumed that automatic quantification of the aortic root complex will facilitate the dynamic analysis of the aortic root complex in the future.

according Hagendorff et al. J Am Coll Cardiol Img 2018; in press

GLOBAL CARDIOLOGY SCIENCE & PRACTICE

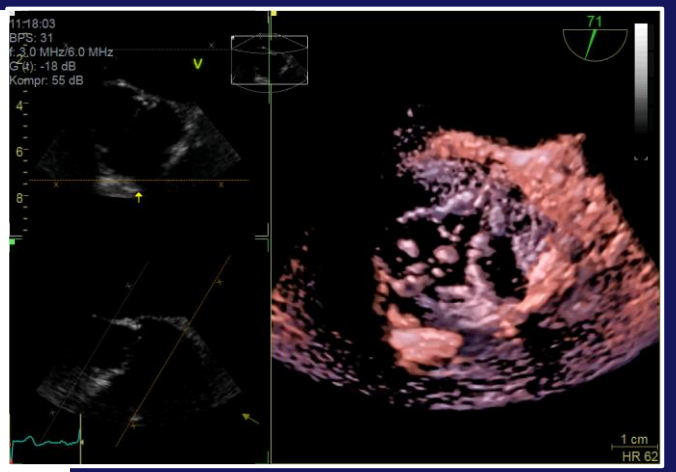

Review article

A systematic approach to 3D echocardiographic assessment of the aortic root

Andreas Hagendorff[1], Stephan Stoebe[1], Bhupendar Tayal[2]

[1] Dep. of Cardiology, University Hospital Leipzig, Germany
[2] Dep. of Cardiology, Aalborg University Hospital, Denmark
*Email: Andreas.Hagendorff@medizin.uni-leipzig.de

Hagendorff et al., Global Cardiology Science and Practice 2018:12
http://dx.doi.org/10.21542/gcsp.2018.12

Advanced Course of Reconstruction of the Aortic Valve and Root: A Practical Approach

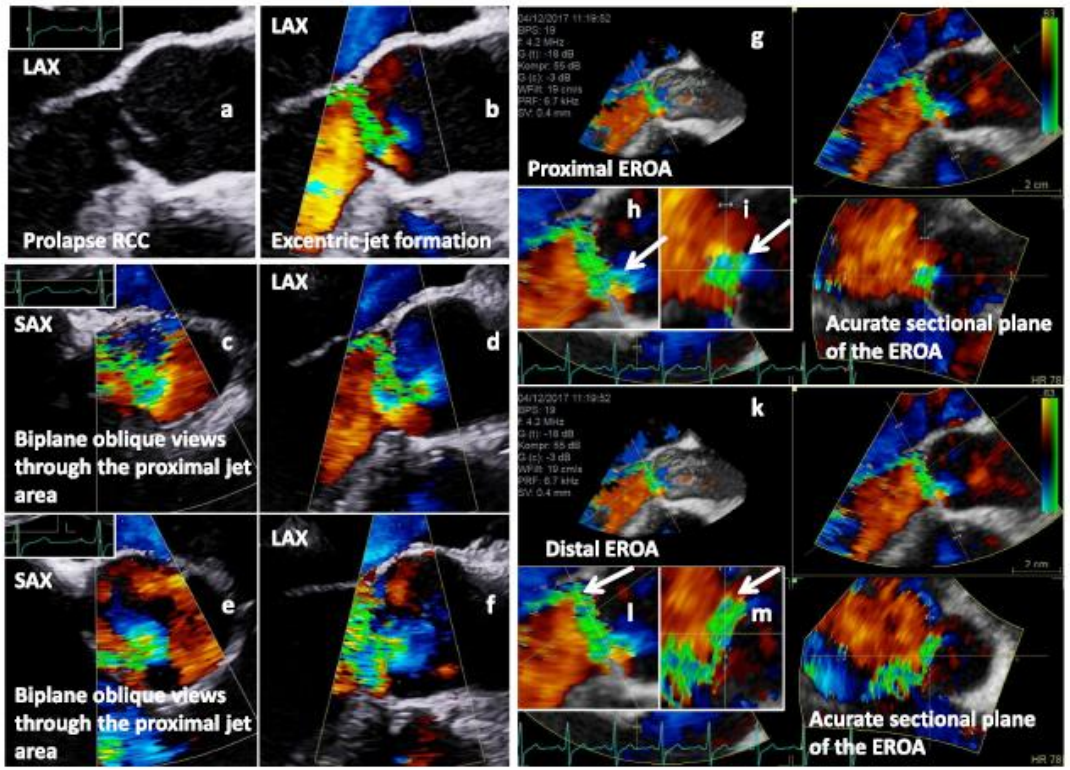

Figure 2. Assessment of the EROA by 2D-echocardiography (a-f) and 3D-echocardiography (g-m); simultaneous long axis view (LAX) of an AV prolapse during diastole (a - native; b - color-coded); color-coded biplane views of the regurgitant jet documenting oblique sectional planes of the regurgitant area in the short axis view (SAX) (c - SAX; d - LAX); second biplane color-coded approach to document the regurgitant jet area (e - SAX; f - LAX); 3D analysis of the entry of the regurgitant jet by post-processing of 3D data sets (g), longitudinal documentation of the central jet formation (h) and accurate perpendicular sectional plane for determination of proximal EROA (i); 3D analysis of the exit of the regurgitant jet by post-processing of 3D data set (k), longitudinal documentation of the central jet formation (l) and accurate perpendicular sectional plane for determination of distal EROA (m).

Optimal and transparent objective analysis of aortic regurgitant orifice area by 3D-echocardiography

Hagendorff et al., Global Cardiology Science and Practice 2018:12
http://dx.doi.org/10.21542/gcsp.2018.12

3D- and Multidimensional Echocardiography in Aortic Valve Repair

Additional information and better diagnostic impact: Quantification of an excentric regurgitation in biscuspid aortic valve ERO - 0.1-0.2 cm^2

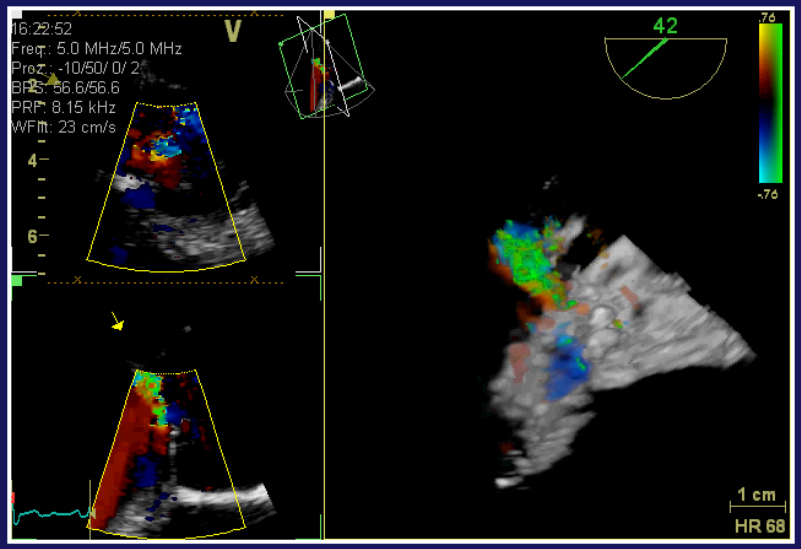

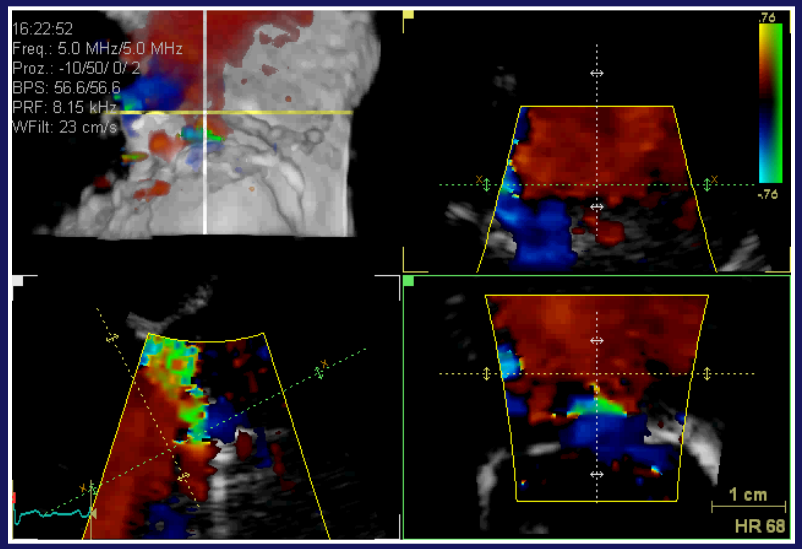

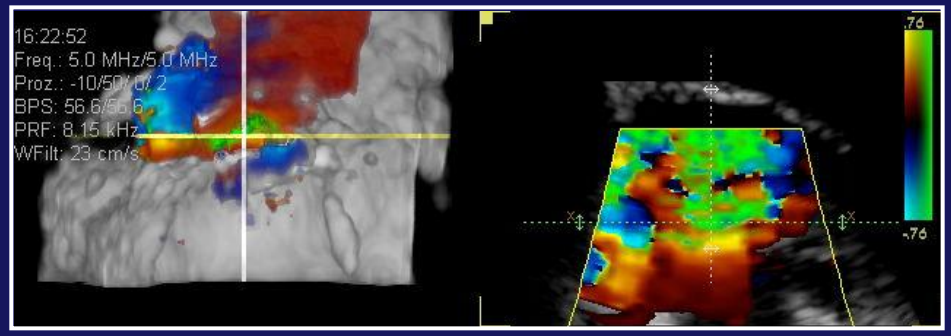

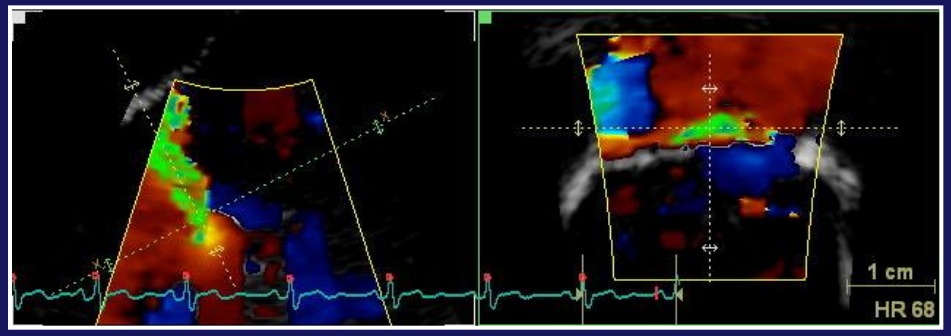

Advanced Course of Reconstruction of the Aortic Valve and Root: A Practical Approach

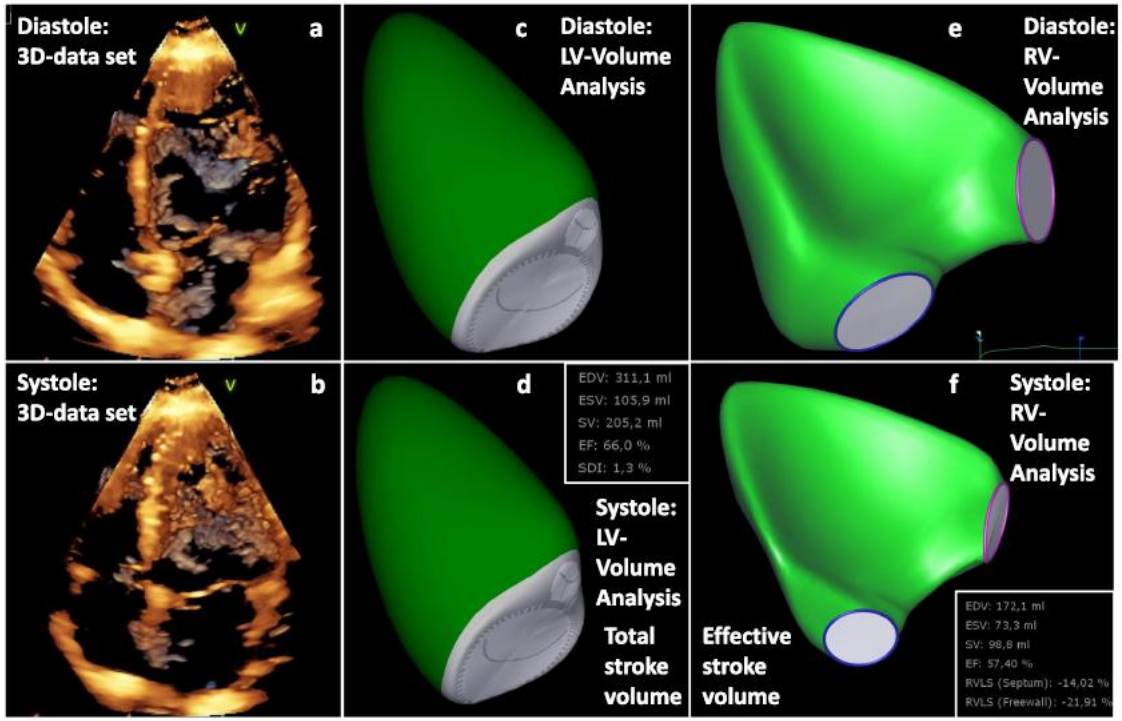

Figure 3. Determination of regurgitant fraction (RF) by 3D-echocardiography. 3D 4-chamber view during diastole (a) and systole (b); determination of LV volumes and total stroke volume (SV_t) by post-processing of 3D data set during diastole (c) and systole (d); determination of RV volumes and effective stroke volume (SV_e) by post-processing of 3D-data set during diastole (e) and systole (f); RF is calculated by $RF[\%] = [(SV_t - SV_e)/SV_t] \times 100$.

3D-analysis of left and right ventricular volumes to determine total, effective and regurgitant volume by 3D echocardiography

Hagendorff et al., Global Cardiology Science and Practice 2018:12
http://dx.doi.org/10.21542/gcsp.2018.12

Advanced Course of Reconstruction of the Aortic Valve and Root: A Practical Approach

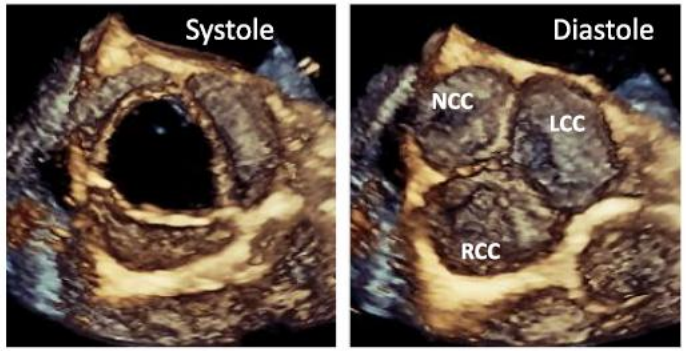

Crown-like ring of the insertion of the cusp at the wall of the VA- junction and the sinus of Valsalva

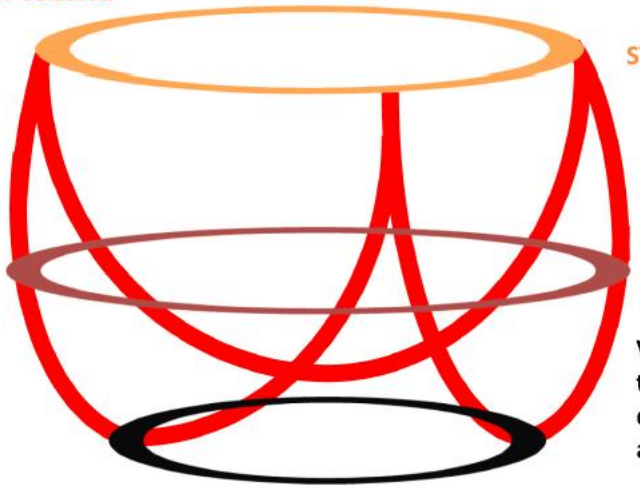

ST junction

Maximum Diameter of Sinus of Valsalva

VA junction at the level of the „hinge points“ determining the virtual aortic anulus

Figure 4. Simplified scheme of the aortic root showing the level of the sinotubular (ST) junction, the maximum diameter of the sinuses of Valsalva, and the ventriculo-arterial (VA) junction at the hinge points of the cusps. The crown-like ring of the cusps insertion with the aortic root is depicted. En-face views of the AV are shown during systole and diastole.

Complex 3D-analysis of the aortic valve and aortic root by 3D echocardiography

Hagendorff et al., Global Cardiology Science and Practice 2018:12
http://dx.doi.org/10.21542/gcsp.2018.12

Advanced Course of Reconstruction of the Aortic Valve and Root: A Practical Approach

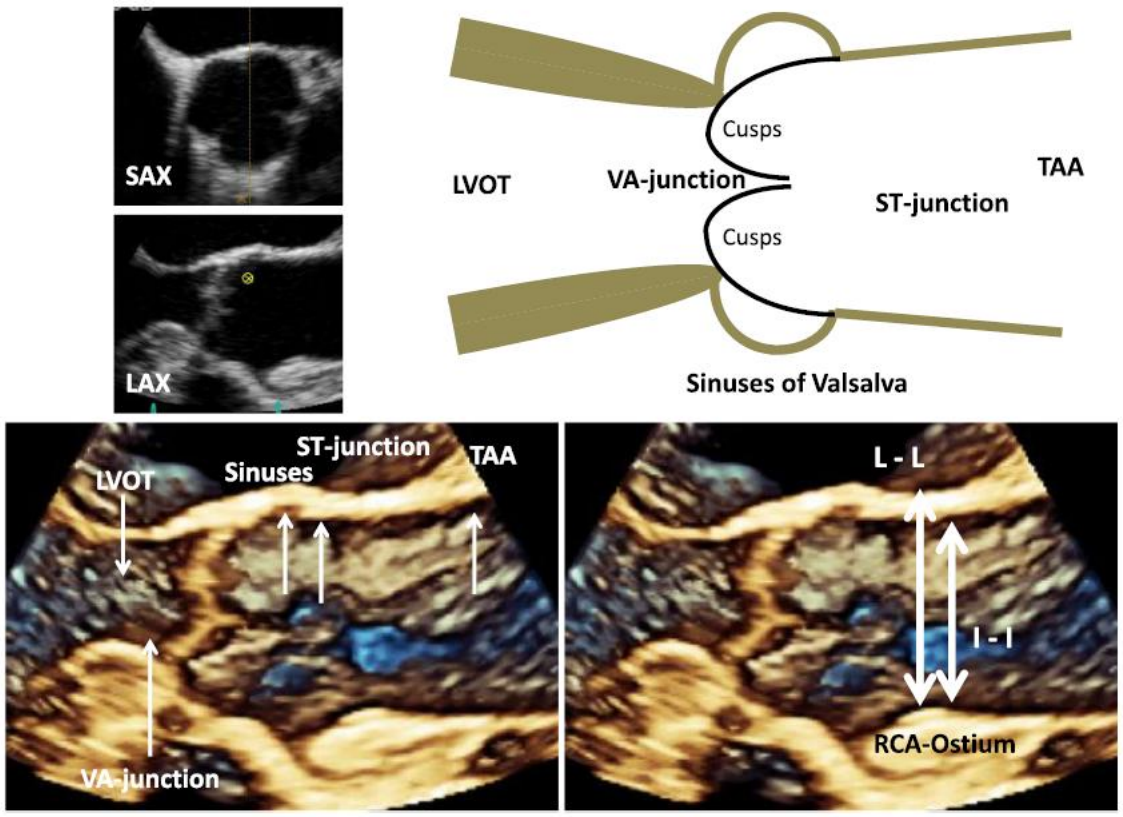

Figure 5. Scheme of the LVOT and the aortic root including 3D TEE-Illustrations of the AV and the aortic root during diastole (left below). The characteristic structures are labeled by white arrows (abbreviations see text). The differences between leading edge to leading edge (L-L) and inner edge to inner edge (I-I) are documented for the diameter of ST-junction (right below).

3D- visualization of the specific cardiac structures

Hagendorff et al., Global Cardiology Science and Practice 2018:12
http://dx.doi.org/10.21542/gcsp.2018.12

Advanced Course of Reconstruction of the Aortic Valve and Root: A Practical Approach

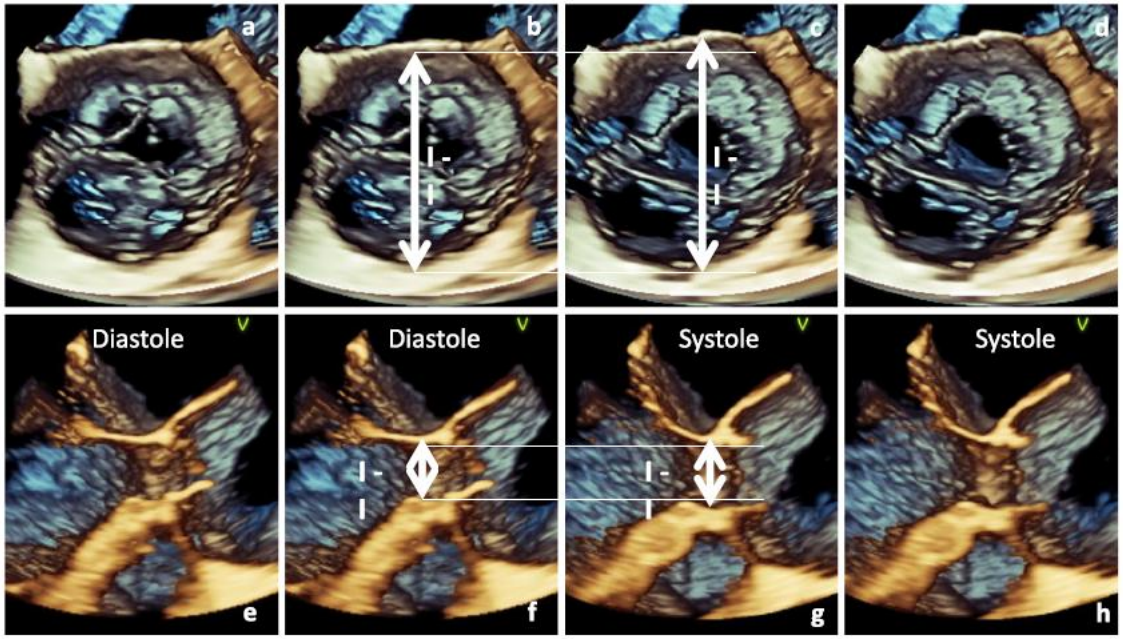

Figure 6. Documentation of the changes of the ST-junction (a-d) and VA-junction (e-h) diameter in a patient with an aneurysm of the ascending aorta and severe aortic regurgitation. En-face view of the AV from the level of the ST-junction is shown at end-diastole (a) including I-I diameter (b); En-face view of the AV from the level of the ST-junction is shown at mid-systole (d) including I-I diameter (c); the difference of the ST-junction diameter is illustrated by dotted lines. Longitudinal view of the AV valve and VA-junction is shown at end-diastole (e) including I-I diameter (f); Longitudinal view of the AV and VA-junction is shown at mid-systole (h) including I-I diameter (g); the difference of the VA-junction diameter is illustrated by dotted lines.

Dynamics of the aortic annulus and the aortic root between diastole and systole. The dimensions are larger during systole than during diastole.

Hagendorff et al., Global Cardiology Science and Practice 2018:12 http://dx.doi.org/10.21542/gcsp.2018.12

Advanced Course of Reconstruction of the Aortic Valve and Root: A Practical Approach

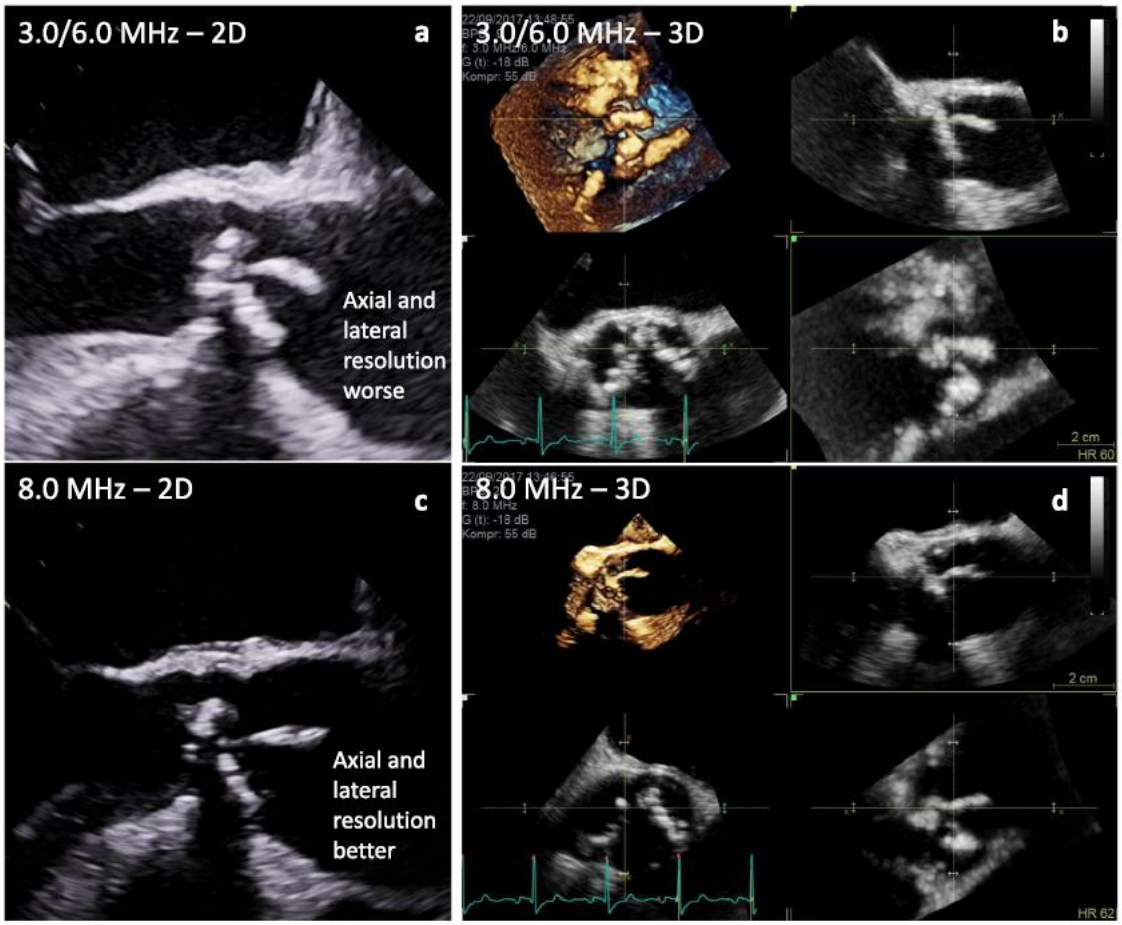

Figure 9. Differences of spatial resolution depending on frequency settings - long axis views (a, c) and 3D data sets (b, d) using low frequencies (harmonic 3.0/6.0 MHz - a, b) and high frequencies (8.0 MHz - c, d) in a patient with endocarditis.

Differences of spatial resolution due to different ultrasound settings – in a case of vegetations at the aortic valve . Thus, settings have to be standardized to be comparable.

Hagendorff et al., Global Cardiology Science and Practice 2018:12 http://dx.doi.org/10.21542/gcsp.2018.12

Advanced Course of Reconstruction of the Aortic Valve and Root: A Practical Approach

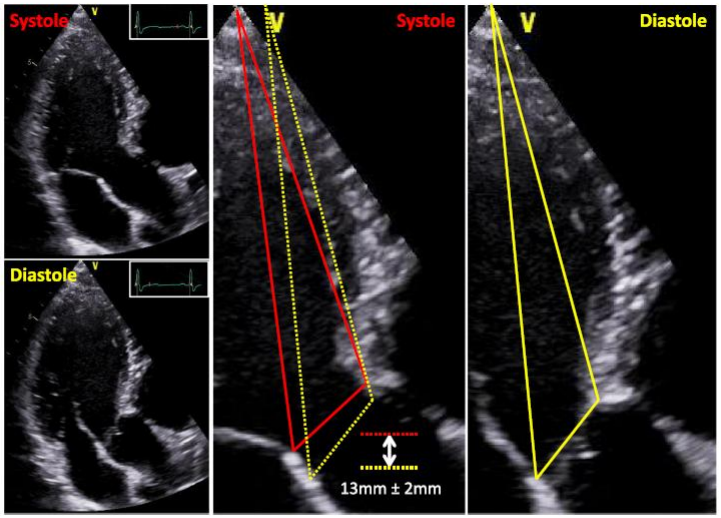

Figure 10. Caudal-cranial aortic annulus excursion between systole and diastole. Due to LV filling during diastole the distance between apex and AV-junction is more cranial in comparison to end-systole. Changes of aortic annulus position are illustrated by yellow lines during diastole and red lines during systole.

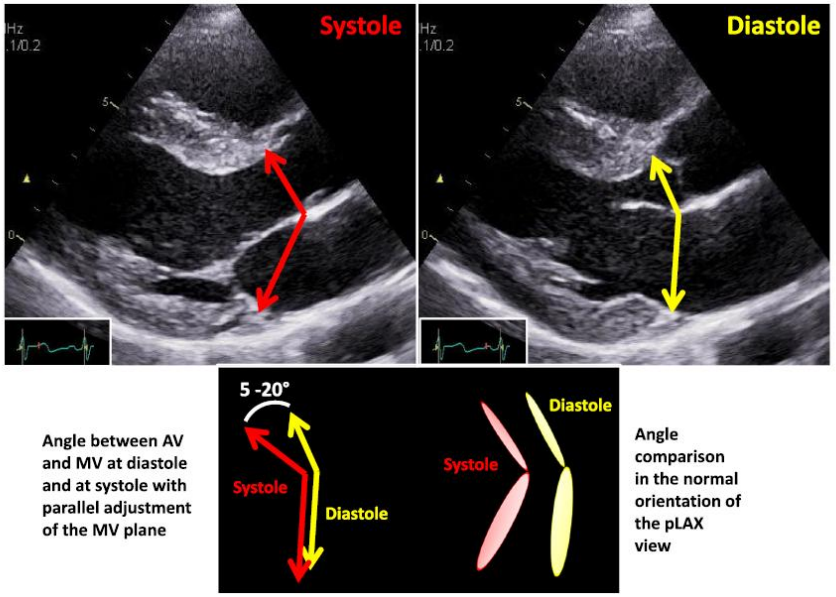

Figure 11. Angle differences between mitral and aortic annulus during systole (red) and diastole (yellow) including a scheme showing the angle difference of the mitral valve during systole and diastole (left below) with parallel adjustment in comparison to normal orientation of the annulus planes (right below).

Documentation of the dynamics
between the mitral and aortic annulus between systole and diastole

Hagendorff et al., Global Cardiology Science and Practice 2018:12 http://dx.doi.org/10.21542/gcsp.2018.12

Advanced Course of Reconstruction of the Aortic Valve and Root: A Practical Approach

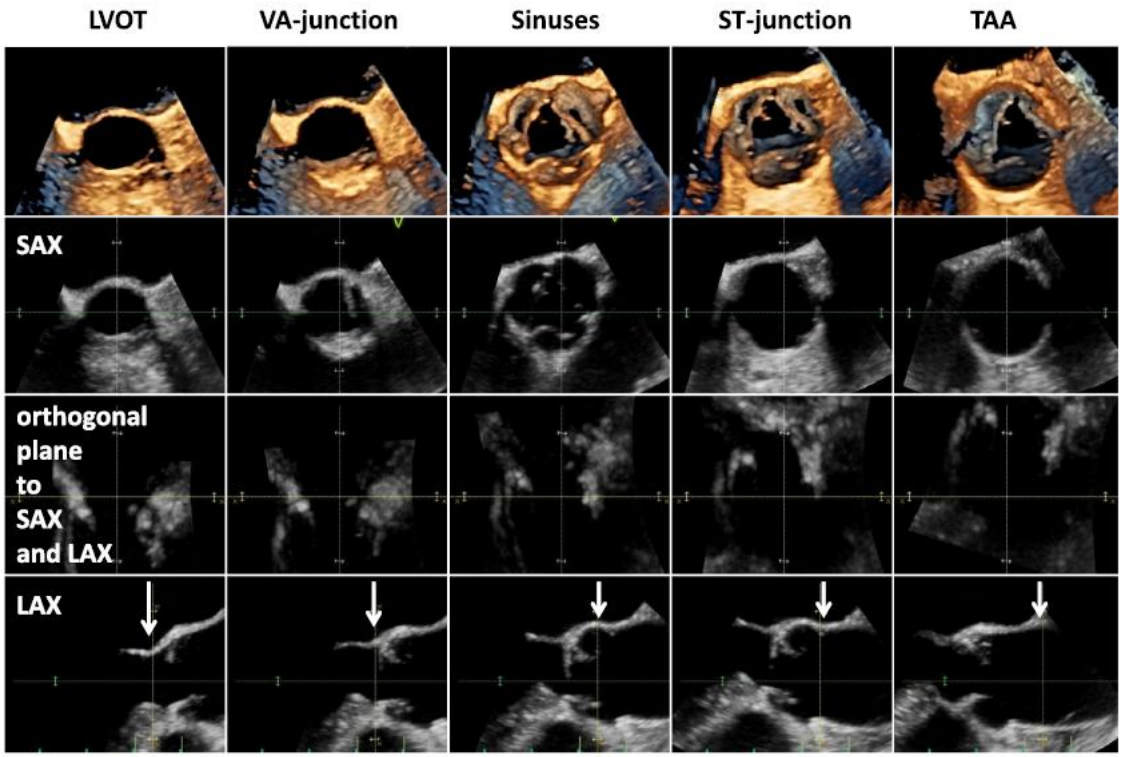

Figure 12. 3D data set with correct adjustment of the cardiac structures during mid-systole for accurate measurement of the aortic root diameter. In the first line 3D short axis views against the bloodstream of the LVOT, VA-junction, sinuses of Valsalva, ST-junction and tubular ascending aorta (TAA) are shown. The second line shows corresponding sectional planes of the short axis views in the 3D data set. The third line shows corresponding horizontal views and the fourth line shows corresponding perpendicular long axis views of the aortic root for the correct measurements of cardiac dimensions labeled by white arrows.

Acurate, transparent and objective measurements of all cardiac structures by 3D-echocardiography

Hagendorff et al., Global Cardiology Science and Practice 2018:12
http://dx.doi.org/10.21542/gcsp.2018.12

Advanced Course of Reconstruction of the Aortic Valve and Root: A Practical Approach

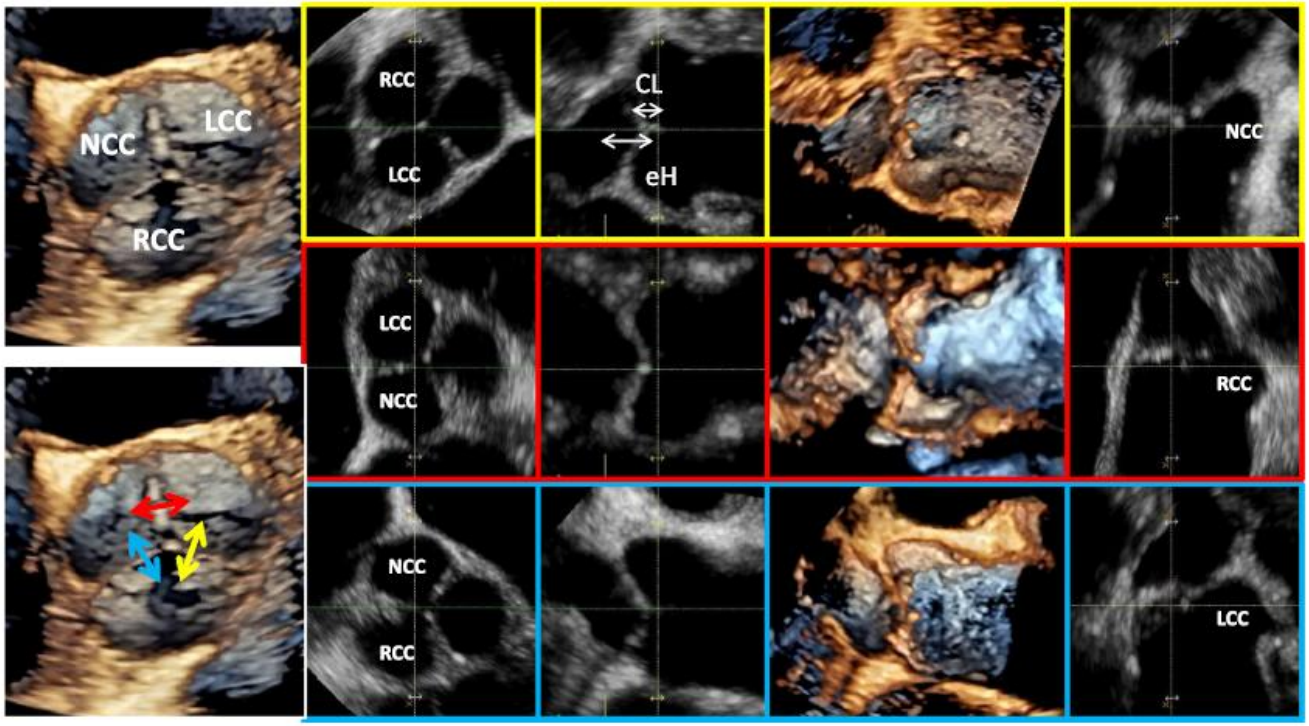

Figure 13. On the left side an en-face view of a normal tricuspid AV is shown. The yellow highlighted images (first line) show the post-processing of correct sectional planes for measurement of CL and eH between the RCC and LCC, the red highlighted images (second line) show corresponding post-processing analysis of CL and eH between the LCC and NCC and the blue highlighted images (third line) show corresponding post-processing analysis of CL and eH between the NCC and RCC.

Measurements of coaptation length and effective height by 3D-echocardiography

Hagendorff et al., Global Cardiology Science and Practice 2018:12 http://dx.doi.org/10.21542/gcsp.2018.12

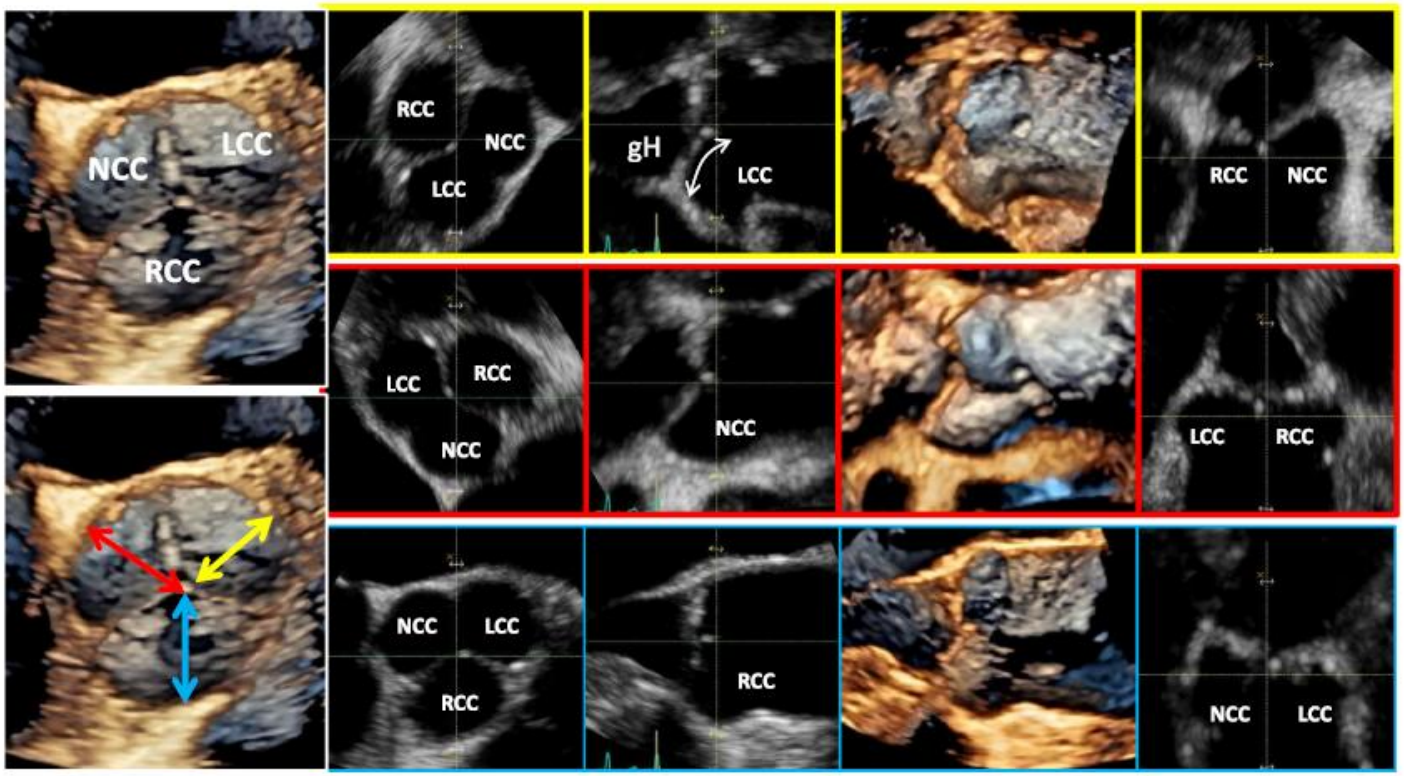

Figure 14. On the left side above an en-face view of a normal tricuspid AV is shown. The yellow highlighted images (first line) show the post-processing of correct sectional planes for measurement of gH of the LCC, the red highlighted images (second line) show corresponding post-processing analysis of gH of the NCC and the blue highlighted images (third line) show corresponding post-processing analysis of gH of the RCC.

Measurements of geometric height by 3D-echocardiography

Hagendorff et al., Global Cardiology Science and Practice 2018:12 http://dx.doi.org/10.21542/gcsp.2018.12

Advanced Course of Reconstruction of the Aortic Valve and Root: A Practical Approach

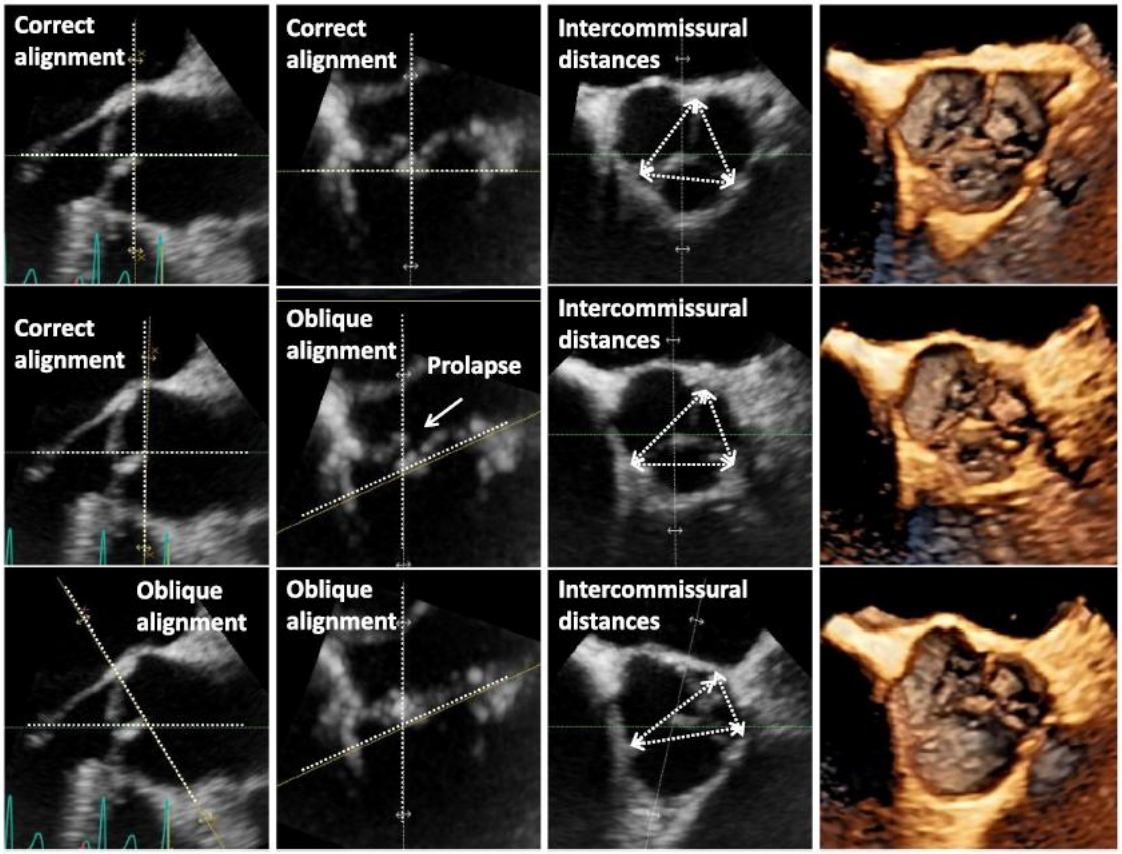

Figure 15. Analysis of the aortic root in correct sectional planes for the determination of the asymmetry by measurements of the intercommissural distances in a patient with prolapse of the NCC. In the first line symmetry of the aortic root is documented by en-face view of the AV displayed by perpendicular planes for adjustment of a correct short axis view parallel to the VA-junction. In the second line an oblique horizontal sectional plane is shown causing significantly different intercommissural distances. In the third oblique horizontal sectional planes and short axis sectional planes are shown causing again misleading measurements.

Acurate, transparent and objective measurements of intercommissural distances by 3D-echocardiography

Hagendorff et al., Global Cardiology Science and Practice 2018:12 http://dx.doi.org/10.21542/gcsp.2018.12

3D- and Multidimensional Echocardiography in Aortic Valve Repair

AI Class	Type I Normal cusp motion with FAA dilatation or cusp perforation				Type II Cusp Prolapse	Type III Cusp Restriction
	Ia	Ib	Ic	Id		
Mechanism	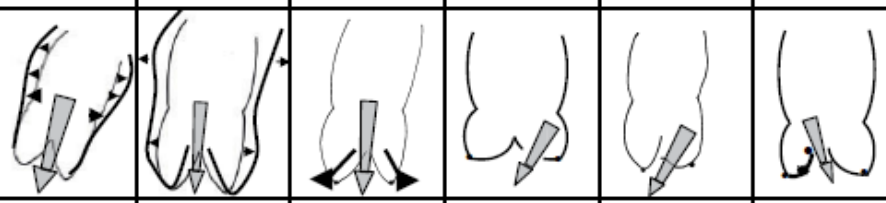					
Repair Techniques (Primary)	STJ remodeling *Ascending aortic graft*	Aortic Valve sparing: *Reimplantation or Remodeling with SCA*	SCA	Patch Repair *Autologous or bovine pericardium*	Prolapse Repair *Plication* *Triangular resection* *Free margin Resuspension* *Patch*	Leaflet Repair *Shaving* *Decalcificatio* *Patch*
(Secondary)	SCA		STJ Annuloplasty	SCA	SCA	SCA

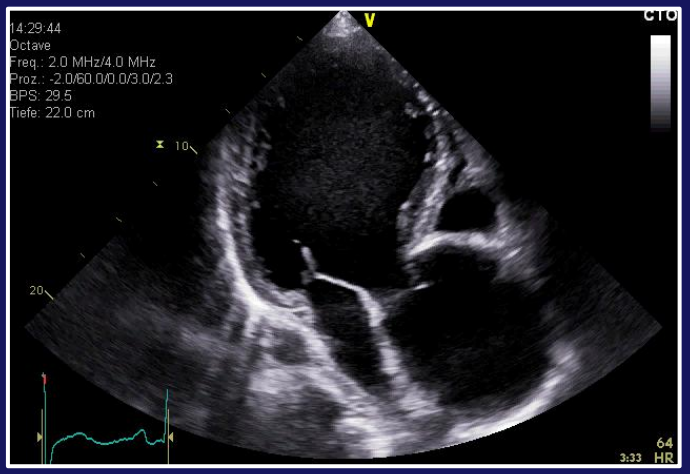

Example of 2D-imaging
Aortic regurgitation type Ia
FAA – functional aortic annulus;
STJ - sinotubular junction;
SCA - subcommissural anuloplasty

Conclusion: Aortic valve repair is an acceptable therapeutic option for patients with aortic insufficiency. This functional classification allows a systematic approach to the repair of AI and can help to predict the surgical techniques required as well as the durability of repair. Restrictive cusp motion (type III), due to fibrosis or calcification, is an important predictor for recurrent AI following AV repair.

Repair-oriented classification of aortic insufficiency: Impact on surgical techniques and clinical outcomes

Munir Boodhwani, MD, MMSc, Laurent de Kerchove, MD, David Glineur, MD, Alain Poncelet, MD, Jean Rubay, MD, Parla Astarci, MD, Robert Verhelst, MD, Philippe Noirhomme, MD, and Gébrine El Khoury, MD

Advanced Course of Reconstruction of the Aortic Valve and Root: A Practical Approach

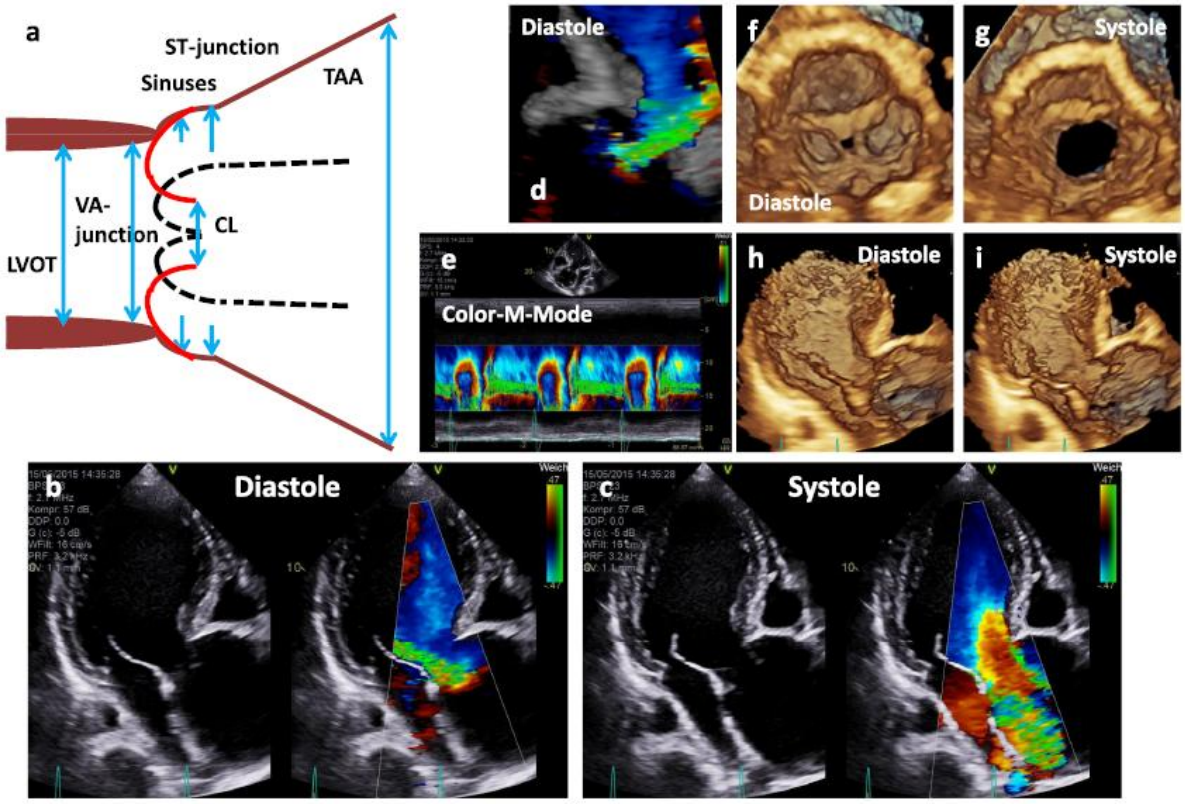

Figure 16. The scheme shows an ectasia of the sinuses of Valsalva and a severe aneurysm of the proximal TAA (a). Below native and color-coded 2D transthoracic images are shown during diastole (b) and systole (c). In addition, 3D TTE image of the aortic regurgitation during diastole (d), color M-Mode of the regurgitation (e), en-face views of the aortic annulus during diastole (f) and systole (g) and 3D transthoracic images of long axis views during diastole (h) and systole (i) are shown.

Documentation of different types of aortic regurgitation by 3D-echocardiography

Hagendorff et al., Global Cardiology Science and Practice 2018:12 http://dx.doi.org/10.21542/gcsp.2018.12

Advanced Course of Reconstruction of the Aortic Valve and Root: A Practical Approach

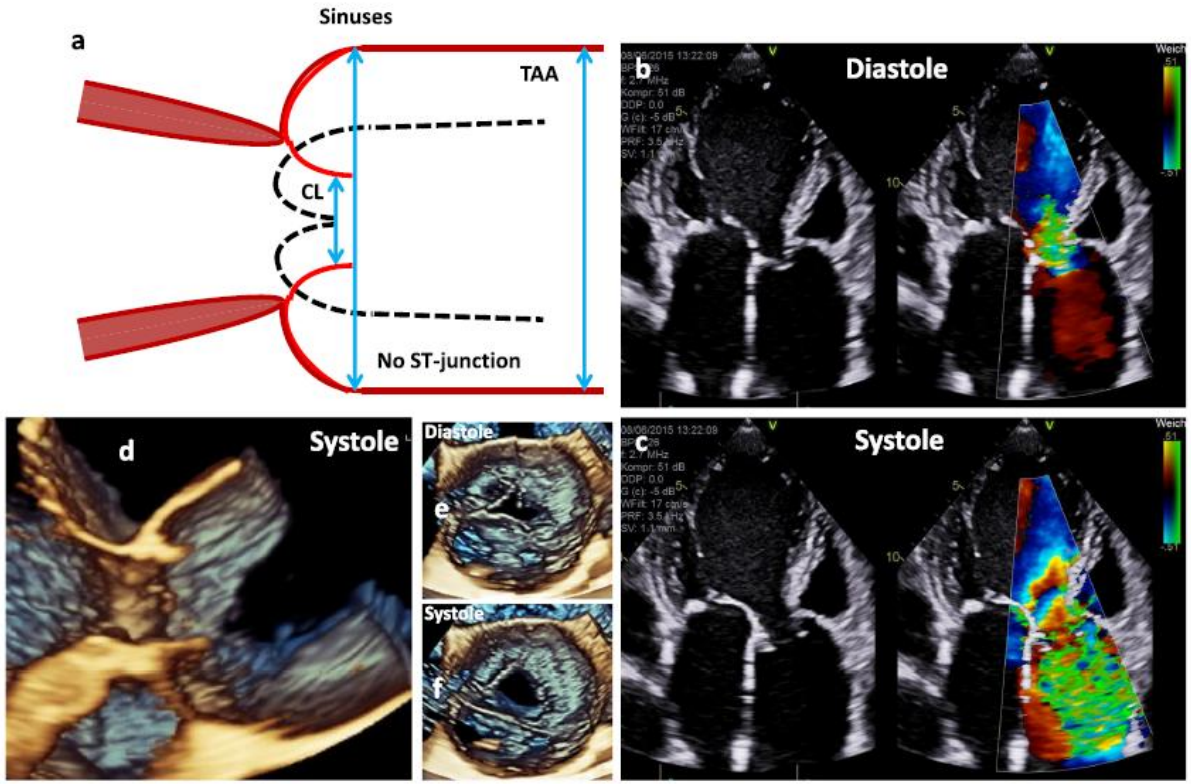

Figure 17. The scheme shows an aneurysm of the sinuses of Valsalva with an ectasia of the proximal ascending aorta and disappearance of the ST-junction and the direct transition of the sinuses into the proximal TAA (a). Further, native and color-coded 2D transthoracic images during diastole (b) and systole (c), 3D transthoracic long axis view during systole (d) and 3D transesophageal en-face views of the AV during diastole (e) and systole (f) are shown.

Documentation of different types of aortic regurgitation by 3D-echocardiography

Hagendorff et al., Global Cardiology Science and Practice 2018:12 http://dx.doi.org/10.21542/gcsp.2018.12

Advanced Course of Reconstruction of the Aortic Valve and Root: A Practical Approach

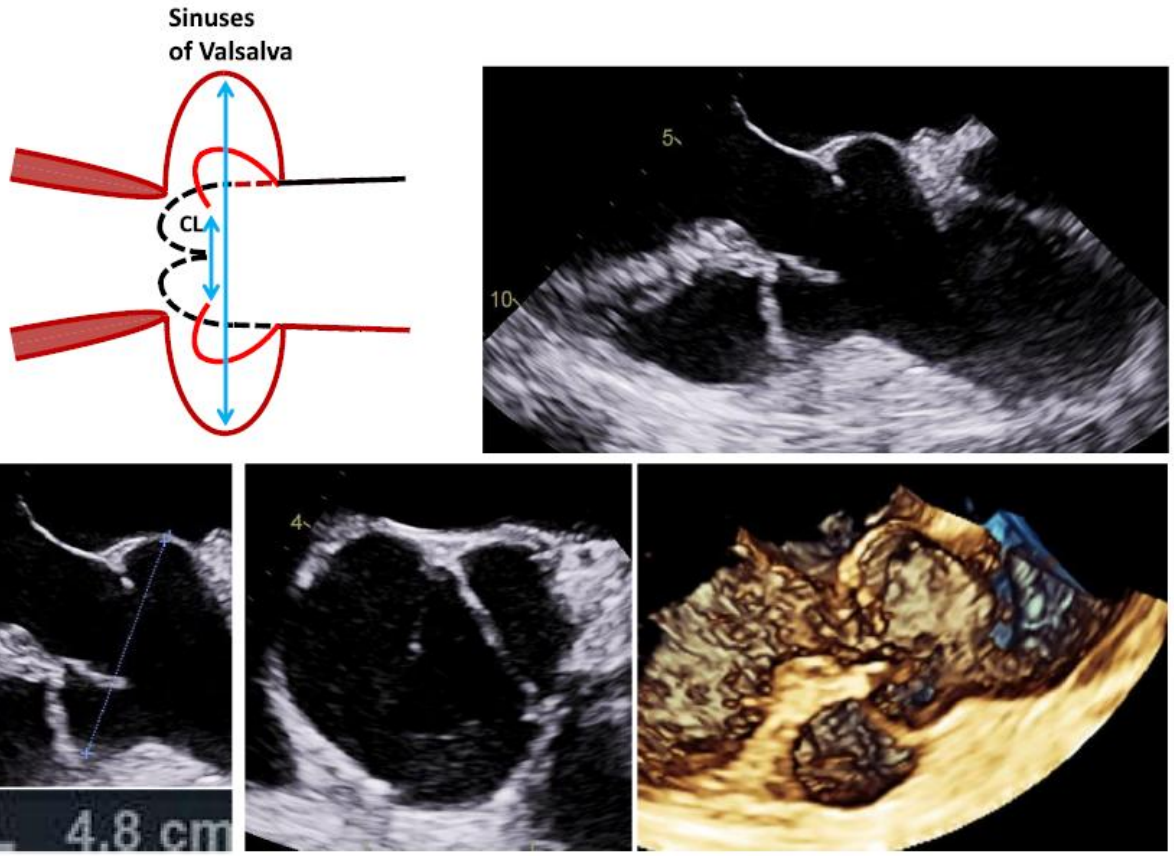

Figure 18. The scheme shows an isolated aneurysm of the sinuses of Valsalva. On the right side and below 2D and 3D transesophageal images during systole as well as the measurement of the aortic root diameter are shown.

Documentation of different types of aortic regurgitation by 3D-echocardiography

Hagendorff et al., Global Cardiology Science and Practice 2018:12 http://dx.doi.org/10.21542/gcsp.2018.12

Advanced Course of Reconstruction of the Aortic Valve and Root: A Practical Approach

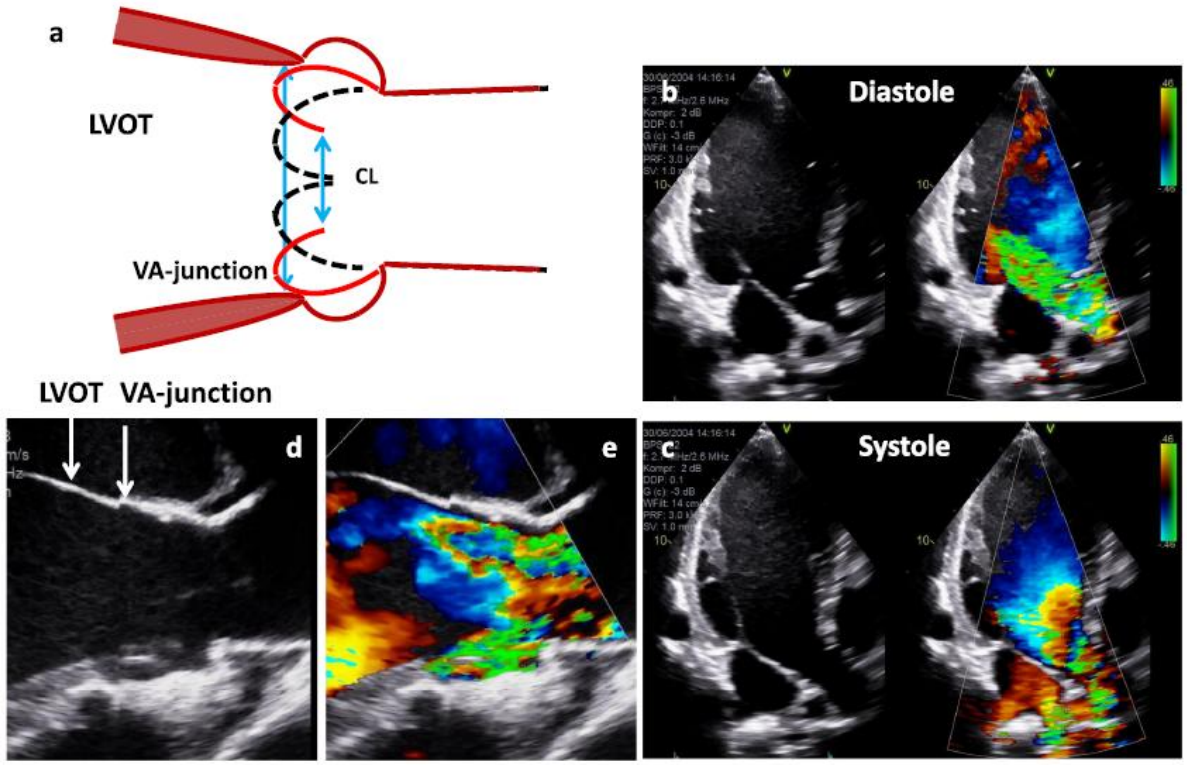

Figure 19. The scheme shows LV dilatation with dilatation of the LVOT and the basal aortic annulus and consecutive severe aortic regurgitation (a). Further, native and color-coded 2D transthoracic images during diastole (b) and systole (c) as well as native (d) and color-coded (e) 2D long axis views of the LVOT and the VA-junction during systole are shown.

Documentation of different types of aortic regurgitation by 3D-echocardiography

Hagendorff et al., Global Cardiology Science and Practice 2018:12 http://dx.doi.org/10.21542/gcsp.2018.12

Advanced Course of Reconstruction of the Aortic Valve and Root: A Practical Approach

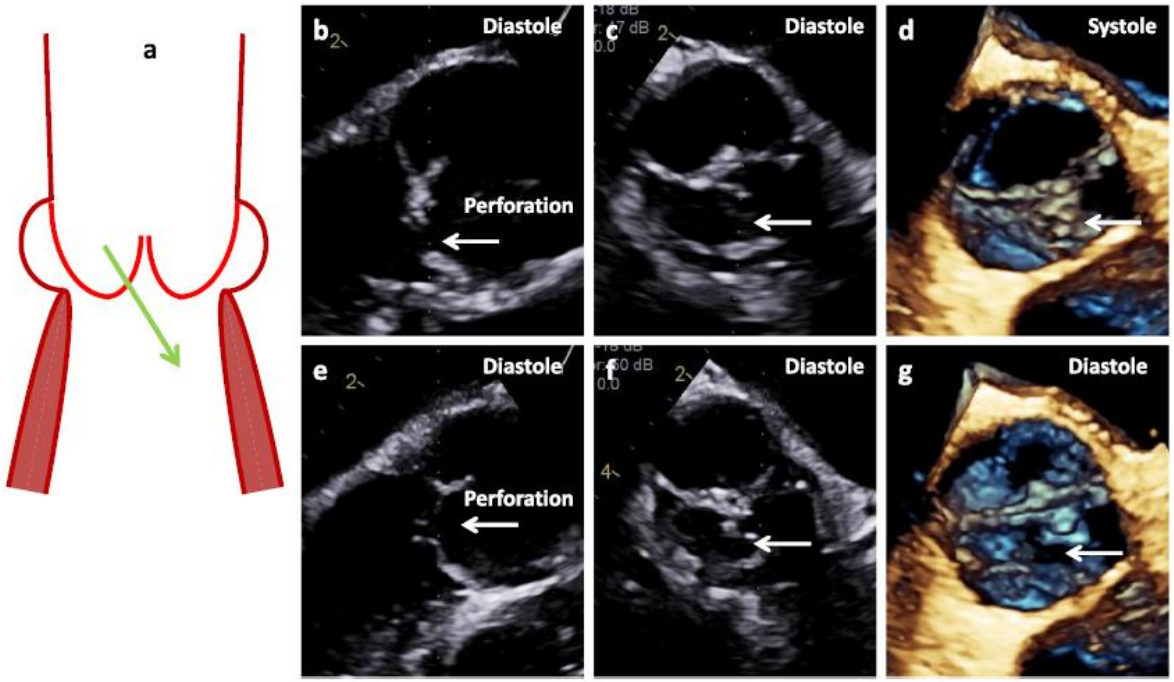

Figure 20. The scheme shows cusp perforation (a). 2D- and 3D images of long axis views (b, e), short axis views (c, f) and 3D-en-face views of the AV (d, g) show perforation of the RCC labeled by white arrows.

Documentation of different types of aortic regurgitation by 3D-echocardiography

Hagendorff et al., Global Cardiology Science and Practice 2018:12 http://dx.doi.org/10.21542/gcsp.2018.12

Advanced Course of Reconstruction of the Aortic Valve and Root: A Practical Approach

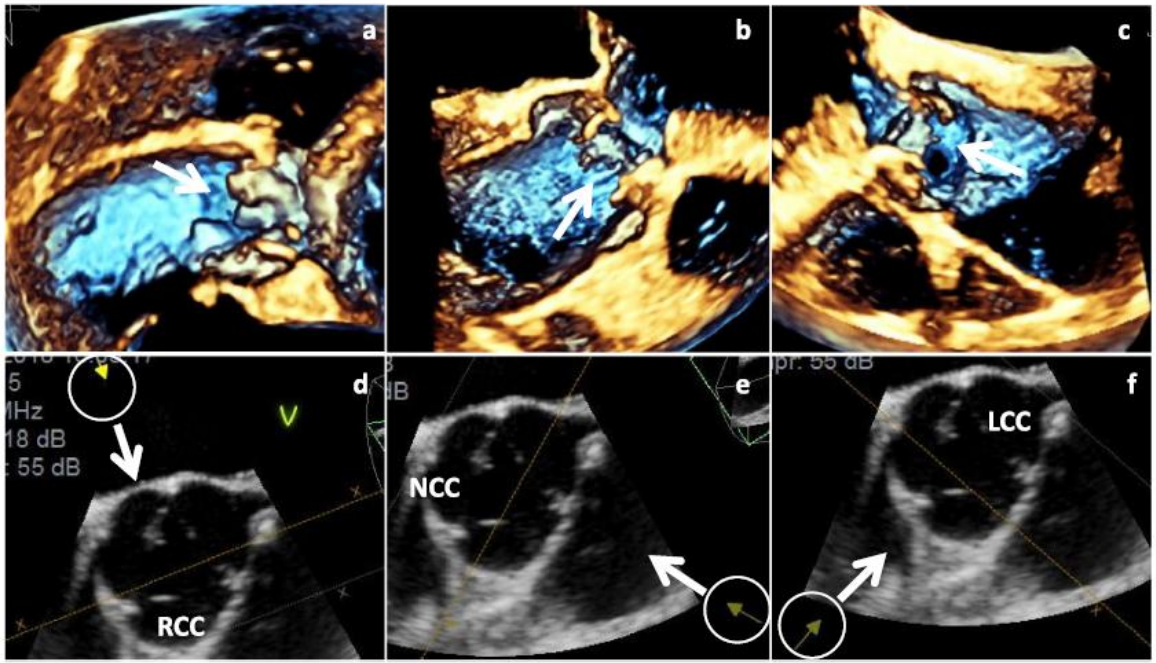

Figure 21. Fenestrations at the margins of the RCC (a), the NCC (b) and the LCC (c) are shown by 3D transthoracic echocardiography. The inhomogeneities of the cusp margin are labeled by white arrows. Below the orientation of the views are given by arrows in corresponding 2D short axis views (d-f).

Documentation of fenestrations at the aortic cusps by 3D-echocardiography

Hagendorff et al., Global Cardiology Science and Practice 2018:12 http://dx.doi.org/10.21542/gcsp.2018.12

Advanced Course of Reconstruction of the Aortic Valve and Root: A Practical Approach

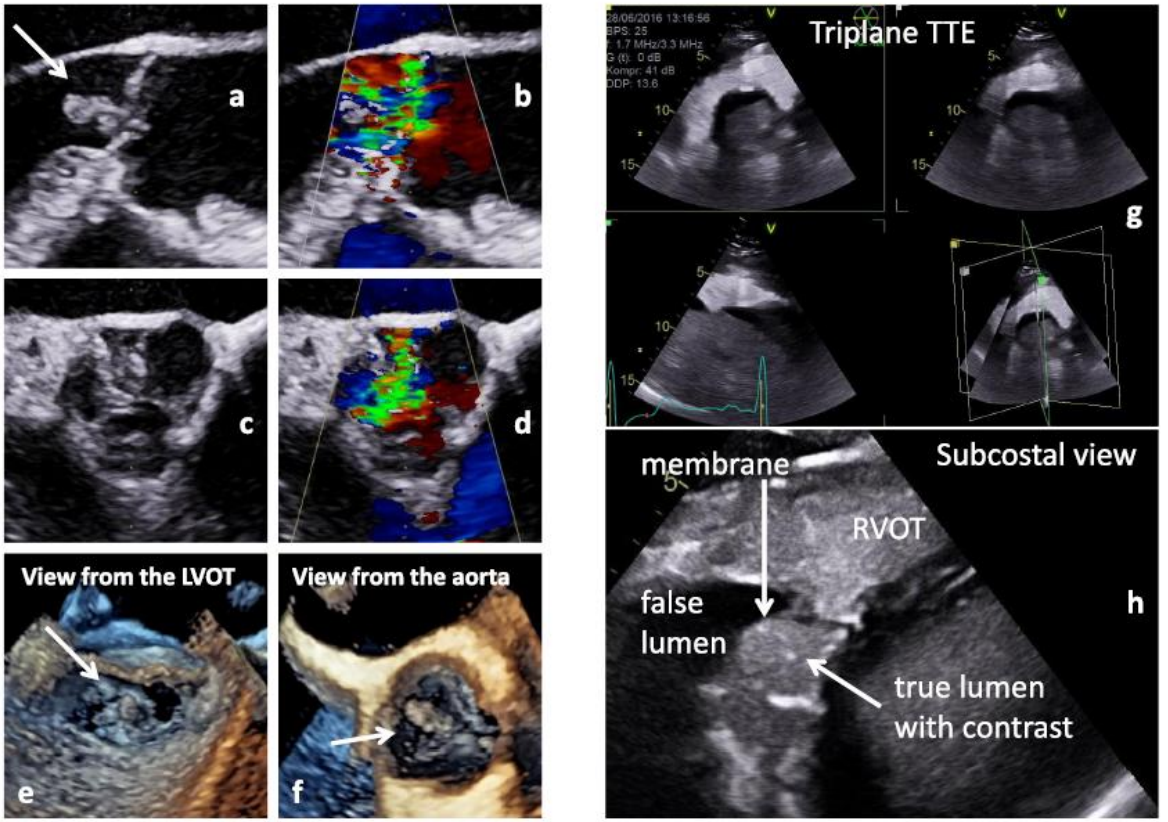

Figure 22. Documentation of vegetations due to endocarditis in native and color-coded 2D transthoracic long axis views (a, b) and 2D transesophageal short axis views (c, d) as well as 3D transesophageal en-face views of the AV from the LVOT (e) and the tubular ascending aorta (f). On the right side aortic dissection (Stanford A) is documented in a triplane subcostal view using contrast echocardiography (g) and in a zoom view of the dissection membrane (h).

Documentation of complications (endocarditis, aortic dissection) by 3D-echocardiography and contrast echocardiography

Hagendorff et al., Global Cardiology Science and Practice 2018:12 http://dx.doi.org/10.21542/gcsp.2018.12

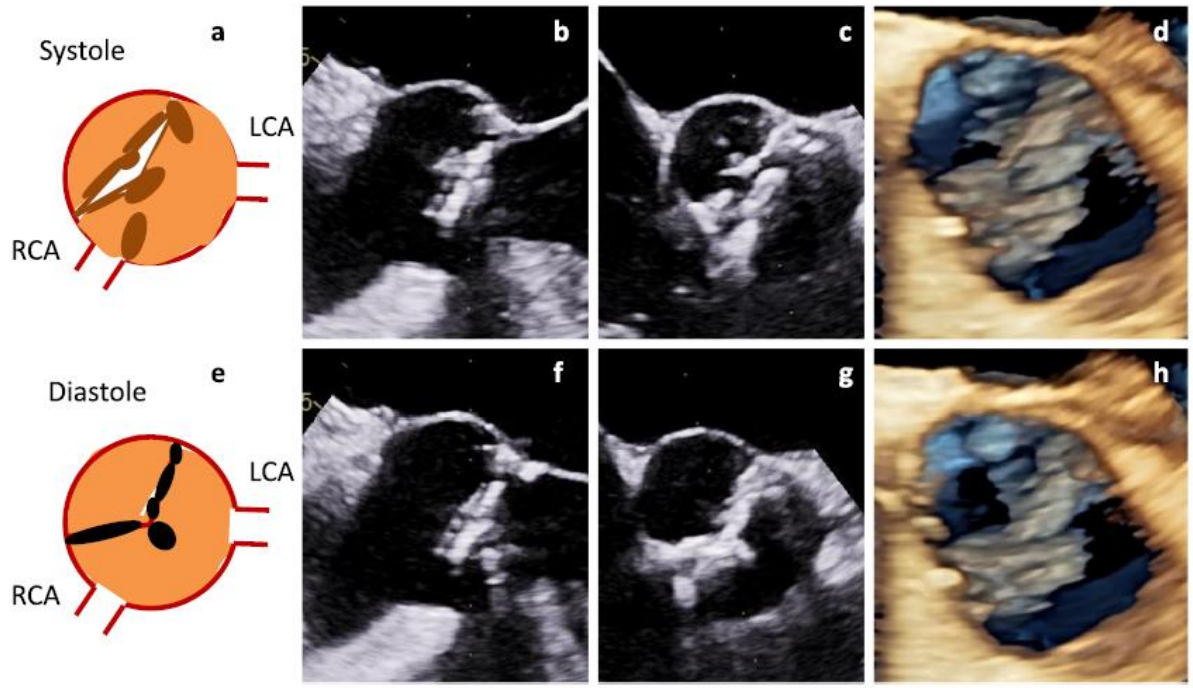

Figure 23. Calcification and retraction of the cusps in a patient with a true bicuspid AV. Scheme of the short axis view (a), 2D transesophageal long axis view (b), 2D transesophageal short axis view (c) and 3D transesophageal en-face view of the AV (d) are shown above during systole. Corresponding views are shown below during diastole (e-h).

Documentation of calcifications and retraction by 3D-echocardiography

Hagendorff et al., Global Cardiology Science and Practice 2018:12
http://dx.doi.org/10.21542/gcsp.2018.12

Advanced Course of Reconstruction of the Aortic Valve and Root: A Practical Approach

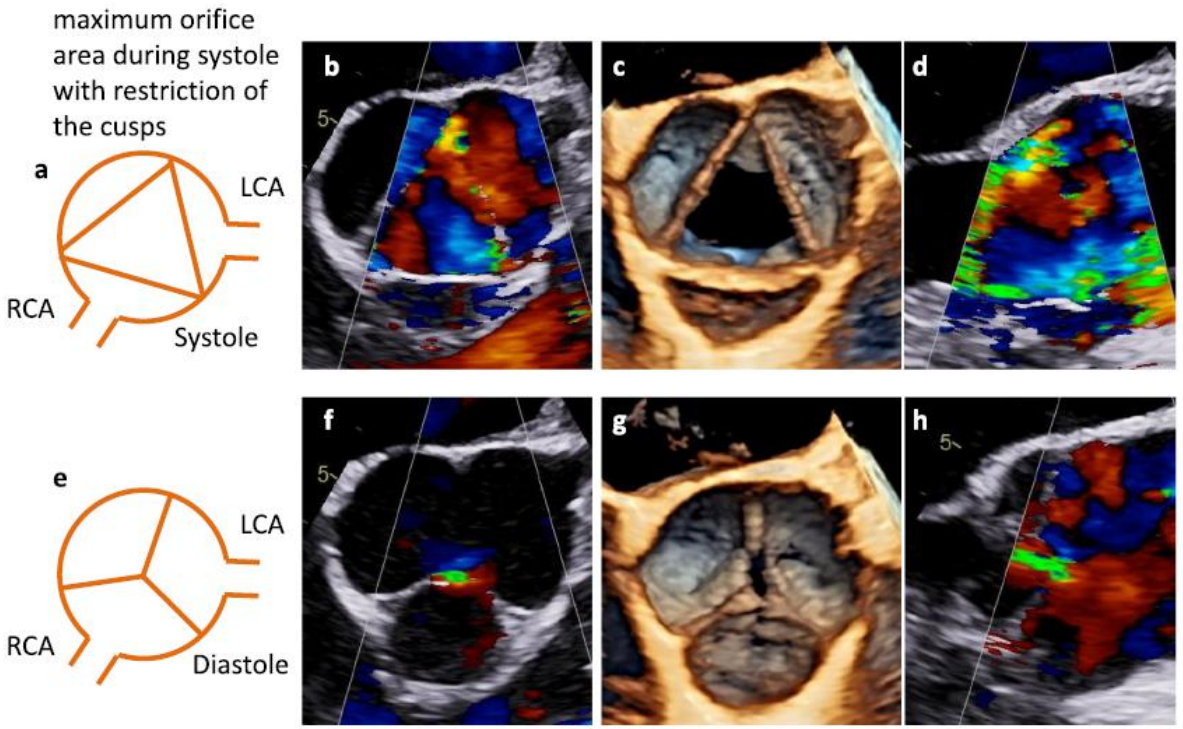

Figure 24. Cusp tethering and functional cusp restriction - tethering is described by reduced geometric cusp height. Scheme of the short axis view (a), color-coded 2D transesophageal short axis view (b), 3D transesophageal en-face view of the AV (c) and color-coded 2D transesophageal long axis view (d) are shown above during systole. Corresponding views are shown below during diastole (e-h).

Documentation of cusp tethering and cusp restriction by 3D-echocardiography

Hagendorff et al., Global Cardiology Science and Practice 2018:12 http://dx.doi.org/10.21542/gcsp.2018.12

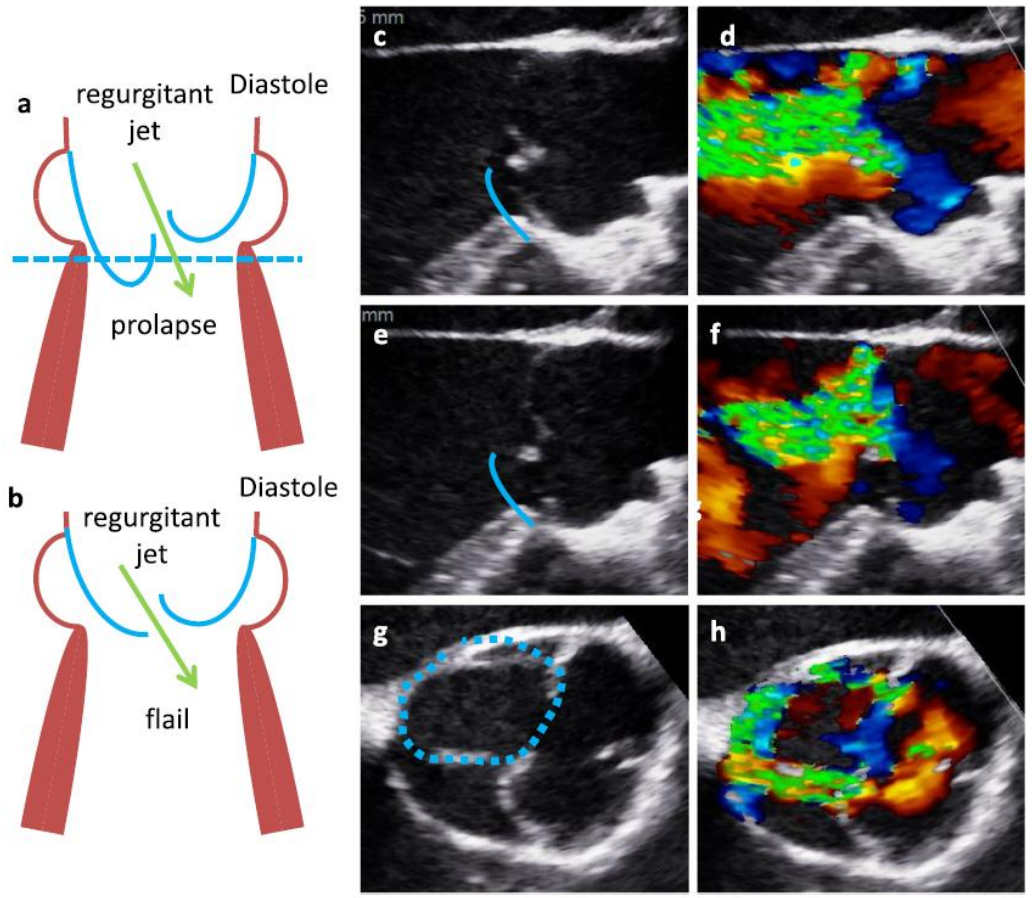

Figure 25. In the scheme a prolapse (a) and a flail (b) are shown in long axis views. On the right side native (c) and color-coded 2D transesophageal long axis view is shown documenting the free margin of the RCC in the LVOT during diastole and the regurgitant jet. Below oblique corresponding views are shown. The course of the RCC and the prolapse are labeled by the blue lines in the native 2D transesophageal images. In (g), (h) color coded 2D transesophageal short axis views show the prolaps by the colored contour displayed by the blue dotted line.

Documentation of cusp prolapses by 2D-echocardiography

Hagendorff et al., Global Cardiology Science and Practice 2018:12 http://dx.doi.org/10.21542/gcsp.2018.12

Advanced Course of Reconstruction of the Aortic Valve and Root: A Practical Approach

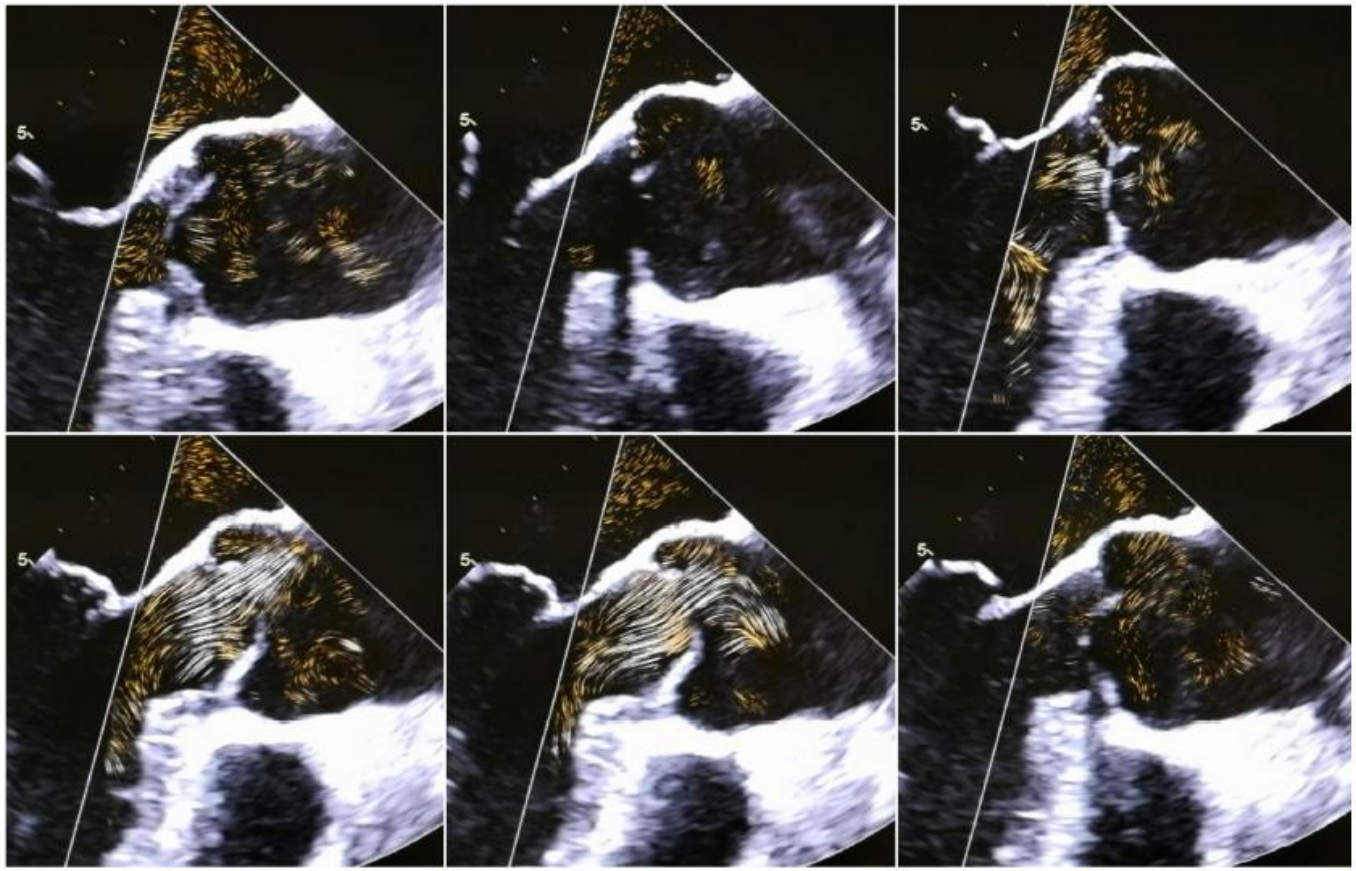

Figure 26. 2D transesophageal long axis views within one cardiac cycle showing the blood flow by blood flow speckle tracking. This new technique permits the visualization of the flow vortex.

Visualization of blood flow turbulences by blood flow speckle tracking

Hagendorff et al., Global Cardiology Science and Practice 2018:12 http://dx.doi.org/10.21542/gcsp.2018.12

SUMMARY

3D-echocardiography should be established in clinical routine to evaluate patients for AV repair and AV-sparing surgery. It is obvious that 3D-transthoracic and transesophageal echocardiography has additional value in characterizing AV and aortic root abnormalities if the image quality of the 3D data sets is sufficient.

The assessment of cusp morphology and function can be best performed by CL, eH and gH, which is possible for all cusps using 3D-echocardiography. Moreover, misleading measurements due to non-standardized, oblique sectional planes can be avoided by 3D-echocardiography.

Thus, 3D-echocardiography should be mandatory for the analysis of AV and aortic root dimensions as well as the grading AR severity. However, sufficient training and experience is required before it can be applied in clinical routine.

Hagendorff et al., Global Cardiology Science and Practice 2018:12 http://dx.doi.org/10.21542/gcsp.2018.12

Multidimensional analysis of aortic arch: Objective measurements of aortic dimensions

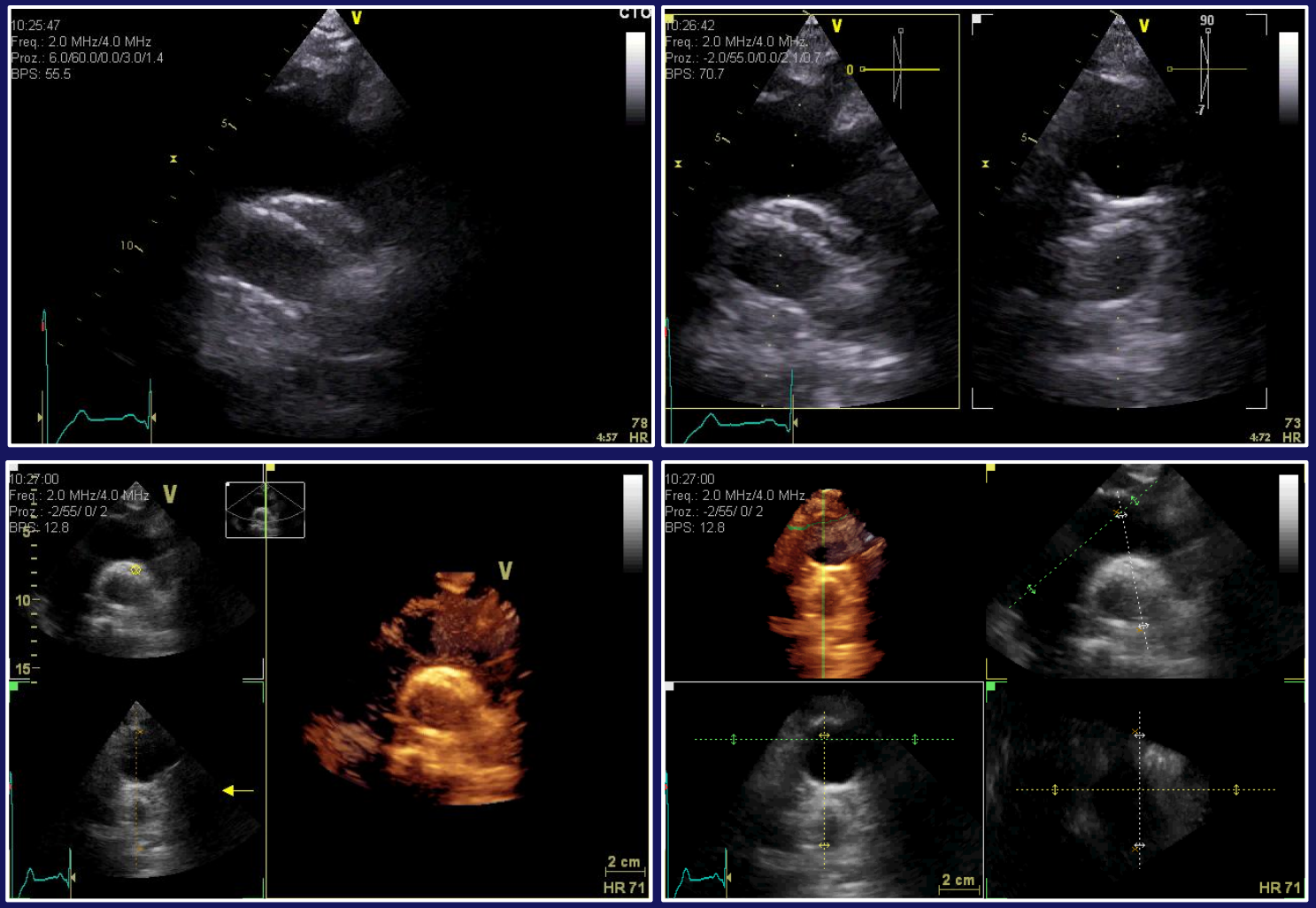

Final Summary:

1. 3D echocardiography enables a completely new modality of imaging in echocardiography – the visualization of surfaces (endocardium and the cusps).
2. Biplane and triplane simultaneous sectional planes enables a better and more acurate standardization of imaging with improvement of measurements of anatomical structures.
3. Postprocessing in 3D data sets offers the possibility of new views (e.g. en-face view of the coronary ostia, etc.)
4. Especially for the decicion making and the planning of the surgical strategy 3D echocardiography can provide important informations.
5. The higher the image quality, the better the information.
6. Thus, training and expertise in 3D echocardiography is a prerequisite for a better diagnosis.

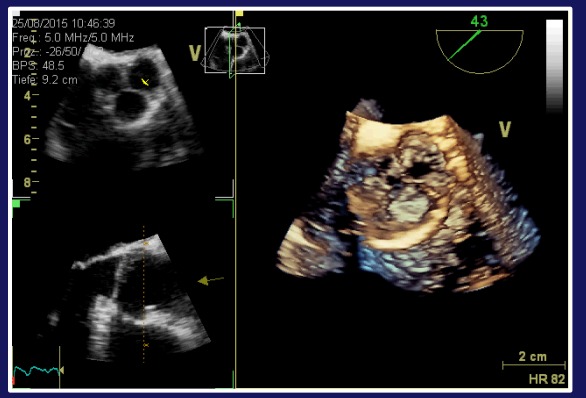

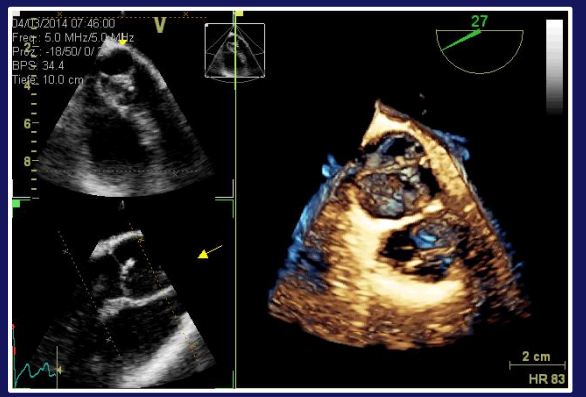

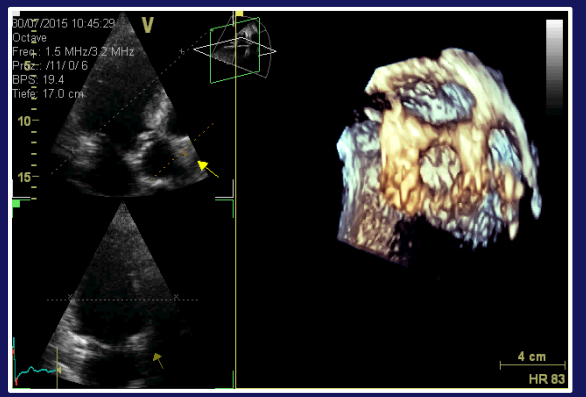

Advanced Course of Reconstruction of the Aortic Valve and Root: A Practical Approach

Siegel der
Universität Leipzig

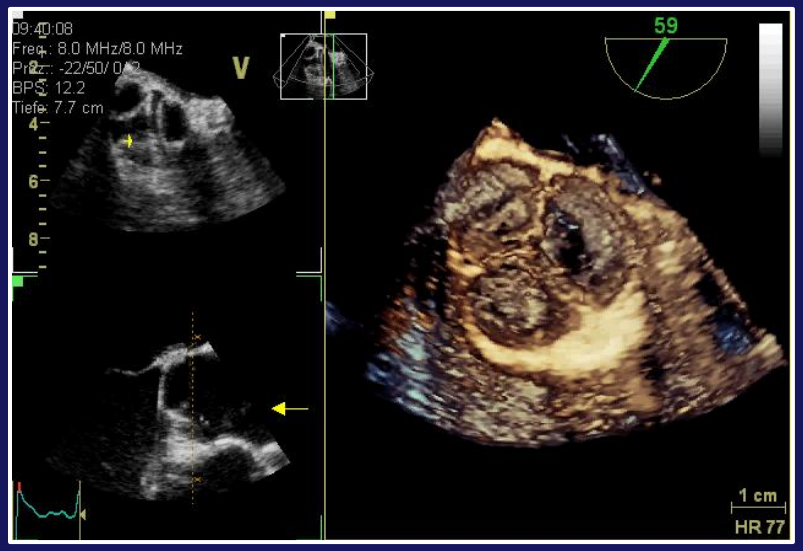

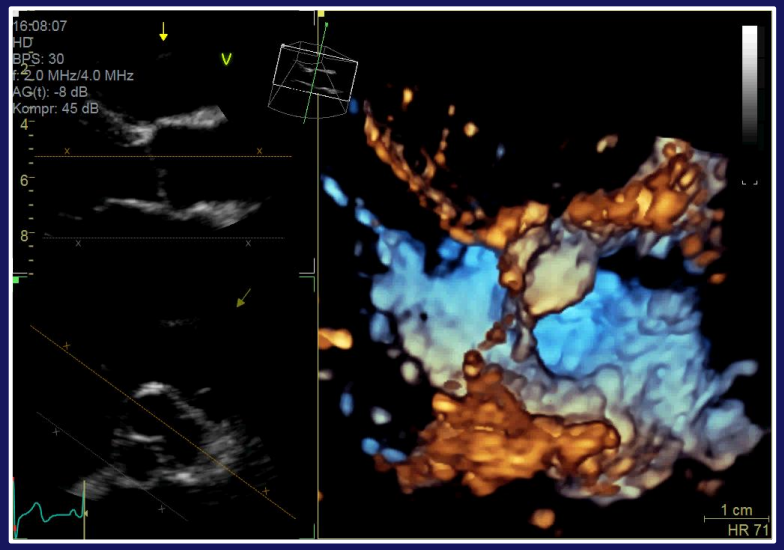

Thank You for Your Attention